

University of Mississippi

eGrove

Electronic Theses and Dissertations

Graduate School

1-1-2019

Investigative study of poly(ionic) liquid incorporation in resin wafer electrodeionization for improved specific energy consumption

Angela Fasuyi

Follow this and additional works at: <https://egrove.olemiss.edu/etd>



Part of the [Engineering Commons](#)

Recommended Citation

Fasuyi, Angela, "Investigative study of poly(ionic) liquid incorporation in resin wafer electrodeionization for improved specific energy consumption" (2019). *Electronic Theses and Dissertations*. 1750.
<https://egrove.olemiss.edu/etd/1750>

This Thesis is brought to you for free and open access by the Graduate School at eGrove. It has been accepted for inclusion in Electronic Theses and Dissertations by an authorized administrator of eGrove. For more information, please contact egrove@olemiss.edu.

INVESTIGATIVE STUDY OF POLY(IONIC) LIQUID INCORPORATION IN RESIN
WAFER ELECTRODEIONIZATION FOR IMPROVED SPECIFIC ENERGY
CONSUMPTION

A Thesis

Presented for the Degree of

Master of Science in Engineering Science

Department of Chemical Engineering

The University of Mississippi

ANGELA AJIBOLA FASUYI

August 2019

Copyright © 2019 by Angela Ajibola Fasuyi

All rights reserved

ABSTRACT

An electrokinetic separation method known as Resin Wafer Electrodeionization (RW-EDI) is recognized as a promising technology for energy efficient desalination of brackish water. However, RW-EDI is limited by an inherent drawback of its ion exchange media that prevents the largescale deployment of this technology. This research was undertaken to optimize the conventional resin wafer used in RW-EDI through the incorporation of high conducting polyionic liquids (PILs). It was hypothesized that by the changing non-conducting polyethylene binder with a PIL binder in conventional resin wafer configurations, ion conductivity within the resin bed would be enhanced, and could lead to an improvement in specific energy consumption (SEC) of RW-EDI. Two different formulations were developed in the fabrication of the phosphonium based PIL-RW and tested in the EDI system at varied applied voltages. The results showed that the amount of PIL used had a significant impact on the mechanical and conductive properties of the resin wafer as well as EDI performance. In the EDI system, a decrease in SEC was achieved when PIL-RW with a reduced PIL/resin ratio was employed, in comparison to conventional polyethylene-based resin wafers. Furthermore, it was concluded that an applied voltage of 6V was optimal for the two-cell pair EDI system.

DEDICATION

This thesis is dedicated to God, through whom all things are possible. I also dedicate this work to my Family for their all-round support and to my loving boyfriend, Nnamdi for being such a wonderful pillar of support throughout my masters' program.

LIST OF ABBREVIATIONS AND SYMBOLS

RO	Reverse Osmosis
ED	Electrodialysis
EDI	Electrodeionization
CEDI	Continuous Electrodeionization
IX	Ion Exchange
AEM	Anion Exchange Membrane
CEM	Cation Exchange Membrane
MF-EDI	Membrane Free Electrodeionization
RW-EDI	Resin Wafer Electrodeionization
IL	Ionic Liquid
PIL	Polyionic liquid
AER	Anion Exchange Resin
CER	Cation Exchange Resin
PE	Polyethylene
PE-RW	Polyethylene-based Resin Wafer

PIL-RW	Polyionic Liquid-based Resin Wafer
PE-EDI	Polyethylene-based Electrodeionization
PIL-EDI	Polyionic Liquid-based Electrodeionization
SEC	Specific Energy Consumption

ACKNOWLEDGMENT

I would like to acknowledge my academic advisor, Dr Alexander Lopez, for his support, mentorship, and patience during my graduate studies.

I would like to acknowledge my committee members, Dr Paul Scovazzo and Dr Brenda Prager for their support and feedback on my research and thesis.

I also wish to acknowledge all the wonderful friends I made while in Oxford, for their unending support and encouragement, as well as my graduate school colleagues who have all been uniquely wonderful.

Finally, special thanks to the University of Mississippi Graduate School for funding this degree.

TABLE OF CONTENTS

ABSTRACT.....	ii
DEDICATION.....	iii
LIST OF ABBREVIATIONS AND SYMBOLS	iv
ACKNOWLEDGMENT.....	vi
TABLE OF CONTENTS.....	vii
LIST OF TABLES.....	x
LIST OF FIGURES	xi
CHAPTER 1	1
1. INTRODUCTION	1
1.1 Global Water Resources	1
1.2 Electrokinetic methods for brackish water desalination: From Electrodialysis to Electrodeionization.....	5
1.3 Ionic Liquids.....	9
1.4 Purpose and Significance.....	12
1.5 Research Objectives	12
CHAPTER 2	14
2. BACKGROUND/LITERATURE REVIEW	14

2.1	Scope of This Chapter	14
2.2	Electrodeionization: Early History and Developments	14
2.3	Theoretical Background	15
2.4	Resin Wafer Technology	21
2.5	Poly(ionic liquid)s as novel materials for ionic conductivity in RW-EDI	23
CHAPTER 3		27
3.	EXPERIMENTAL MATERIALS AND METHODS	27
3.1	Materials and Instrumentation	27
3.2	Synthesis of Ionic Liquid monomer	28
3.3	Wafer Composition and Fabrication.....	30
3.4	EDI Set-Up	31
CHAPTER 4		35
4.	RESULTS AND DISCUSSION.....	35
4.1	Fourier Transform Infrared Spectroscopy	35
4.2	Characterization of Resin Wafer as Ion Conducting Spacers.....	36
4.3	Application in EDI system	39
CHAPTER 5		47
5.	SUMMARY AND CONCLUSION	47

CHAPTER 6	49
6. FUTURE WORK.....	49
LIST OF REFERENCE	50
APPENDIX.....	59
VITAE.....	66

LIST OF TABLES

Table 1-1: Summary of innovative Electrodeionization methods.....	9
Table 3-1: Detailed Specification of Ion Exchange Resins.....	28
Table 3-2: EDI experiment set-up.....	32

Equivalent circuit for determining the special dispersion of current in RW-EDI. (R_B is resistance of the bead, R_C is resistance of the contacting point, R_S is resistance of the solution, R_b is resistance of the boundary layer, R_P is the resistance of the polymer and C_b capacitance of the boundary layer). Modified from [24] 24

Figure 3-1: Synthesis of Trioctyl(4-vinylbenzyl)phosphonium-bis(trifluoromethane)- sulfonimide i.e. $[P888_{(4-VB)}][Tf_2N]$ 29

Figure 3-2: Front view of ElectroCell system showing inlet and outlet ports 32

Figure 3-3: Side view 32

Figure 3-4: Configuration of a Resin Wafer Electrodeionization cell 33

Figure 4-1: IR spectra of IL $[P888VB][TF_2N]$ and PIL Poly $[P888VB][TF_2N]$. The change in C=C stretch at $898-933\text{ cm}^{-1}$ of the polymer shows the degree of polymerization (89% approx..)..... 36

Figure 4-2: Microscope images of PE-RW (1a & 1b), PIL-RW with 3g PIL (2a & 2b) & PIL-RW with 2.5g PIL (3a & 3b) at $\times 4$ and $\times 10$ magnification. I & IV are ion exchange resins, II are Polyethylene clusters around resin beads and III shows two resin beads bound by PIL film. 38

Figure 4-3: Comparisons in average current response and corresponding average removal efficiency of PE-EDI and PIL-EDI (comprising 3.0 g PIL) runs, at 6.5V & 8V. 40

Figure 4-4: Comparing the average removal rate of PE-EDI and PIL-EDI (comprising 3.0 g PIL) runs, at 6.5V and 8V. 40

Figure 4-5: Comparisons in average current response and the corresponding average removal efficiency of PE-EDI and PIL-EDI (comprising 2.5 g PIL) runs, at 6 V & 7V. 41

Figure 4-6: Comparing the average removal rate of PE-EDI and PIL-EDI (comprising 2.5 g PIL) runs, at 6 V and 7 V.	42
Figure 4-7: A comparison of the removal efficiency and SEC at 6.5 V for PE-EDI and PIL-EDI (comprised of 3.0 g PIL) runs.	43
Figure 4-8: A comparison of the removal efficiency and SEC at 8 V for PE-EDI and PIL-EDI (comprised of 3.0 g PIL) runs.	43
Figure 4-9: A comparison of the removal efficiency and SEC at 6 V for PE-EDI and PIL-EDI (comprised of 2.5 g PIL) runs.	44
Figure 4-10: A comparison of the removal efficiency and SEC at 7 V for PE-EDI and PIL-EDI (comprised of 2.5 g PIL) runs.	44
Figure 4-11: A comparison of average current efficiencies for PE-EDI and PIL-EDI runs. PIL-EDI (comprising 3.0 g PIL) is shown as red bars while PIL-EDI (comprising 2.5 g PIL) is shown as green bars.....	46

CHAPTER 1

1. INTRODUCTION

1.1 Global Water Resources

1.1.1 Water demand and production

Water is an essential resource on earth which sustains all aspects of human existence. Two thirds of the earth's surface is covered by water of which 97% is seawater, and the remainder available as freshwater. Daily, worldwide consumption of freshwater reaches a total of 10 billion tons [1]. The Food and Agriculture Organization of the United Nations (FAO) reported that freshwater withdrawal increased from 600 km³/yr to 4000 km³/yr globally within the last century [2]. Water for agricultural uses accounted for about 70 percent of the total consumption, followed by industrial (16 to 20 percent) and municipal (9 to 14 percent) consumers [3]. However, over the past few decades, there has been a significant reduction in water supply around the globe. This scarcity has been linked to water stresses triggered by the effects of climate change. At the same time, water demand has increased drastically, owing to high population density as well as industrialization. As these sectors continue to grow and expand, the global water demand is projected to increase 40% by 2020, prompting the need for alternative water sources to augment current supply [4].

1.1.2 Production methods & Limitations

Since 1999, developing new sources of freshwater and managing current demand has been the focus of many research studies [5–9]. Saline and reclaimed water are some of the non-traditional sources being explored as sustainable solutions to alleviate water stresses. These sources include seawater, brackish water, and wastewater (from cooling towers, oil and gas activities, thermoelectric plants, mining activities and agricultural activities). Although seawater is largely available, access to its sources is limited to coastal areas. On the other hand, brackish water/wastewater reuse is a growing efficient water resource in arid or inland regions. It is projected that the wastewater market will hit \$11 billion (USD) by 2025 in the US, while global water reuse is expected to increase by a factor of 8 [10]. While these alternative sources of freshwater are capable of adequately meeting current demand, treatment (e.g. desalination) is necessary to ensure fit-for-purpose quality at both utilization and discharge stages. Concerns about energy demands of treatment processes arise when fulfilling stringent water standards. Thus, optimization of energy is important in the deployment of desalination technologies for sustainable water production and management of the food-water-energy nexus.

1.1.3 Desalination methods and limitations

Desalination has been at the focal point of many water reclamation processes, evolving with increasing water quality and quantity demands. Water desalination can be classified into thermally-driven, pressure-driven, and biological-related methods. Traditionally, freshwater was generated from seawater via thermally-driven desalination methods such as multi-effect distillation (MED) and multi-stage flash distillation (MSF) [11,12]. However, operational complexity and high energy

consumption of these thermal desalination technologies led to their gradual replacement by membrane-based systems [13].

Membrane-based desalination technologies offer promising solutions to water treatment challenges because of their high product recovery and low environmental footprint. They account for about 60 percent of the total installed capacity globally [14]. Membrane-based technologies employ semi-permeable membranes to separate undesired species from water, making them useful in sea/brackish water desalination as well as wastewater reclamation. Since the first successful development of cellulose acetate membranes for reverse osmosis (RO) in the 1960s, membrane technology has undergone revolutionary improvements and commercialization for desalination applications. Pressure-driven membrane processes such as Microfiltration (MF), Ultrafiltration (UF), Nanofiltration(NF) and Reverse Osmosis (RO) are now widely used for the removal of biological, organic, inorganic and other pollutants from water/wastewater. RO effectively removes contaminant matter and salts containing 35g/L Total Dissolved Solids (TDS). Additionally, seawater desalination via RO is generally considered to be less energy intensive and more cost-effective than thermally-driven methods. In 2011 [15], RO accounted for 63 percent of the global installed desalination capacity and is still dominating the desalination markets. RO's popularity stems from advancement in membrane materials, improvement in module design, energy reduction among other benefits, which has yielded significant cost reductions than its early days of commercialization. RO continues to be the leading process for seawater desalination but there are associated drawbacks with low salinity feeds that render the technology uneconomical for large scale desalination of brackish water (or water with <10g/L TDS) [16,17]. Some of these disadvantages of RO include low energy efficiency, less than ideal product recovery, and increased brine production.

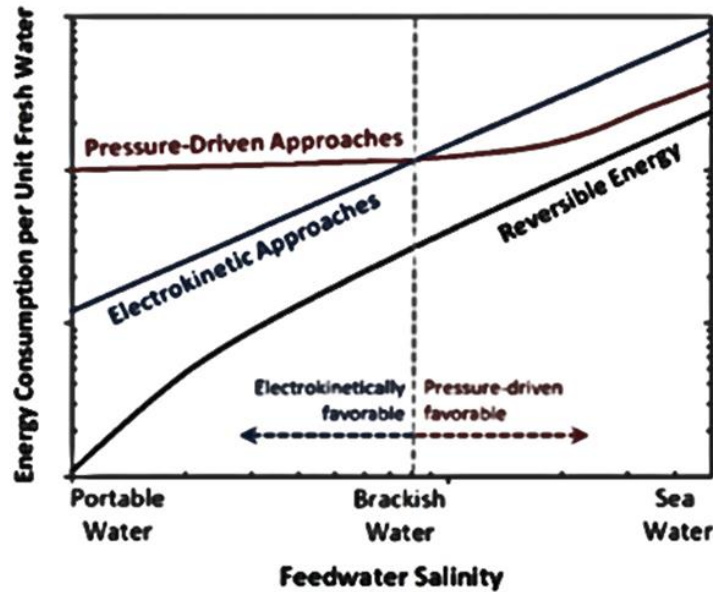


Figure 1-1: Diagram showing energy consumption versus feed water salinity for different desalination technologies [18]

Consequently, there is a shift towards electrically-driven, otherwise known as electrokinetic approaches for brackish water desalination [18]. Electrokinetic technologies are more energy efficient and better suited for removal of ions/salt from low salinity feed than pressure-driven RO as highlighted in **Figure 1-1**. They are categorized into:

- i. Electrosorption such as Capacitive Deionization (CDI),
- ii. Electroseparation methods such as Electrodialysis (ED) and Electrodeionization (EDI).

In ED-based processes, ions migrate via ion exchange membranes under an electric field. Although ED is a mature technology for water purification, it is generally less efficient for the production of low conductivity product streams. This led to the development of an advanced ED process known as Electrodeionization (EDI).

For treatment of low salinity feed, EDI amasses interest because of its competitive advantage over other pressure-driven and electrokinetic separation techniques that typically require costly brine management. Besides water treatment, EDI has the following novelty applications:

- i. Recovery of organic acids from fermentation broths for the production of organic compounds [19,20].
- ii. Extraction of energy from wastewaters containing nitrogen-laden pollutants via a hybrid system of Solid Oxide Fuel Cells and EDI [21].
- iii. CO₂ capture and recovery at atmospheric pressures by the electrochemical pH control of the system [22].
- iv. Selective ion removal in dialysate free artificial kidney devices for the treatment of blood in patients with malfunctioned kidneys [23].

1.2 Electrokinetic methods for brackish water desalination: From Electrodialysis to Electrodeionization

EDI emerged principally from electrodialytic method of separation. An ED system operates on the principles of dialysis and electrolysis, through which ions are separated via semi-permeable ion exchange membranes into two compartments- a dilute (ion depleting) compartment and a concentrate (ion-enriching) compartment. ED systems were originally applied for the demineralization of syrup in 1890 but have been extended to several areas, some of which include: water desalination, organic compound separation, selective removal of ions. Despite the excellent separation capabilities demonstrated by ED, an intrinsic drawback of the process limits the energy efficiency of the system. At low ionic concentration, a phenomenon known as concentration

polarization develops, which occurs when a concentration gradient is established between the membrane surface and the bulk solution, caused by the permselectivity of the membranes. Furthermore, as ions become depleted in the dilute compartment, current density increases with applied voltage until it reaches a threshold. Above this limiting current density (shown in **Figure 1-2**), an increase in the cell's resistance develops. Once this point is reached, any further increase in electrical potential results in dissociation of water into hydrogen H^+ ions and hydroxyl OH^- ions. This effect of concentration polarization inadvertently lowers the efficiency of the ED system.

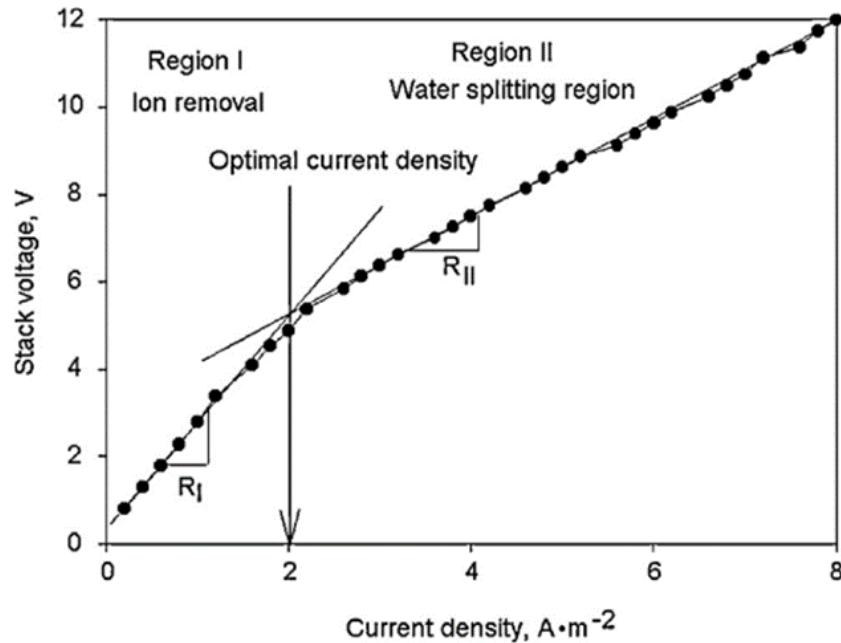


Figure 1-2: Current-voltage curve of the CEDI system [24]

To overcome the limitation of ED, a solid medium (ion exchange resins i.e. 'IX') was introduced into the dilute compartment of the system. Generally, IX resins selectively exchange cations and anions in solution enabled by a chemical potential gradient which exists between the insoluble ion exchange material and the solution. In the ED system, they serve as conductive bridges. In the EDI system, the separation efficiency of electro dialysis and exchange capabilities

of ion exchange is enhanced. The concentration polarization suffered by the ED system is prevented by incorporating resins into the ion depleting compartment. Ion transport within the dilute solution to the membrane is promoted by the resin bed which acts to minimize the cell's electrical resistance. Simultaneously, resins are regenerated in-situ by proton and hydroxyl ions produced from water splitting which occur on the contact sites of anionic and cationic materials, as illustrated in **Figure 1-3**. The electroregeneration of resins eliminates the need for harsh chemical agents as in typical ion exchange processes. Thus, the complementary integration of ED and ion exchange allows for efficient and environmentally friendly treatment of very dilute/low ionic solutions.

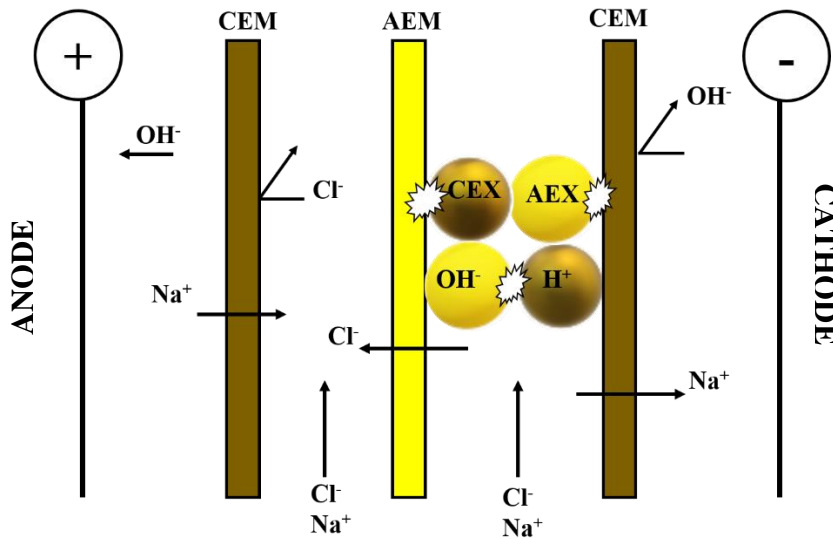


Figure 1-3: Water splitting sites of resins, reproduced from [25]

EDI continuously undergoes optimization and material development for better efficient and novel separation applications [25]. Special ion exchange membranes have been developed for EDI modules to mitigate the drawbacks of insufficient mechanical strength and handling properties in ED membranes. Recent reports on heterogeneous membranes consisting of polyolefin binder

suggested they were more suitable for EDI applications because of their cost effectiveness, flexible formulation and resistance to fouling [26]. Other innovative methods have been proposed to improve the performance of the conductive media in EDI. Membrane-free EDI (MF-EDI) is a fairly recent deionization technology that was developed for high purity water production [27]. Although MF-EDI has a few advantages including fast, effective resin regeneration as well as low energy consumption, it is still yet to be well established for large scale industrial applications. Besides, MF-EDI suffers backward migration of ions caused by its complex regeneration method, which reportedly diminishes product quality [28]. Another key innovation to the EDI unit is the immobilization of ion exchange resins into porous wafers as a way of breaking the barriers of prior configurations. Loose IX resins are confined by means of a binder and formed into a solid porous, pliable wafer. This way, resin-wafer EDI configuration (RW-EDI) effectively minimizes ion leakage even at high flow rates, without impeding in-situ regeneration of resins or the deployment of ions. However, there is an undesired resistance associated with the conventional wafer characteristics, propelling the development of highly conductive resin wafers in EDI systems. In the present work, we aim to achieve this enhancement in resin wafer conductivity through the incorporation of polymer based- ionic liquids. A summary of the advantages and limitations of the innovations to EDI is presented in **Table 1-1**.

Table 1-1: Summary of innovative Electrodeionization methods.

Electrodeionization Technology	Innovation	Advantages
Conventional Electrodeionization	Loosely packed resins in diluate chamber.	Mature Technology. Some limitations include: <ul style="list-style-type: none"> - Potential escaping of resin beads - Ion leakage within compartments - Uneven flow distribution
Membrane-Free Electrodeionization	Only utilizes resins to deionize feed solution.	Still under development. Eliminating membranes prevents potential fouling. Disadvantages include: <ul style="list-style-type: none"> - Regeneration complexity - Backward migration of ions - Low product recovery and quality
Resin Wafer Electrodeionization	Porous wafer- formed by confinement of resins in diluate chamber by polymer binder.	Under development. Small scale commercial applications available. Corrects inefficiencies of EDI and MF-EDI. Some limitations include: <ul style="list-style-type: none"> - Formation of dead zones - Low energy efficiency

1.3 Ionic Liquids

In the last 20 years, ionic liquids (ILs) have increasingly gained attention in the research space. Ionic liquids (ILs) harbor unique properties for application in electrochemistry and untapped potential for electrokinetic separations. They are defined as a class of molten salts with low melting points (typically below 100 °C or ambient temperature). ILs comprise an organic cationic part (such as imidazolium, N-alkyl pyridinium, tetraalkylammonium, and tetraalkylphosphonium ions) and an anionic part which can be organic or inorganic (for example halides, nitrate, acetate, hexafluorophosphate ([PF₆]), tetrafluoroborate ([BF₄]), trifluoromethyl sulfonate ([OTf]), and bis(trifluoromethanesulfonyl)imide ([Tf₂N] moieties) [29], as illustrated in **Figure 1-4**. The

diverse physiochemical properties exhibited by ILs are attributed to their tunable cation and anion combinations, giving rise to a myriad of applications in synthesis, catalysis, ion conduction, lubrication, surfactants etc. In electrically-driven separations, ILs have also found application as liquid membranes and recovery solvents [30,31]. In more recent applications, ILs are used as building blocks of nanostructured materials due to their high charge density. In their liquid state, ionic liquids can be disadvantageous in some applications that require mechanical stability, durability and better processability [32].

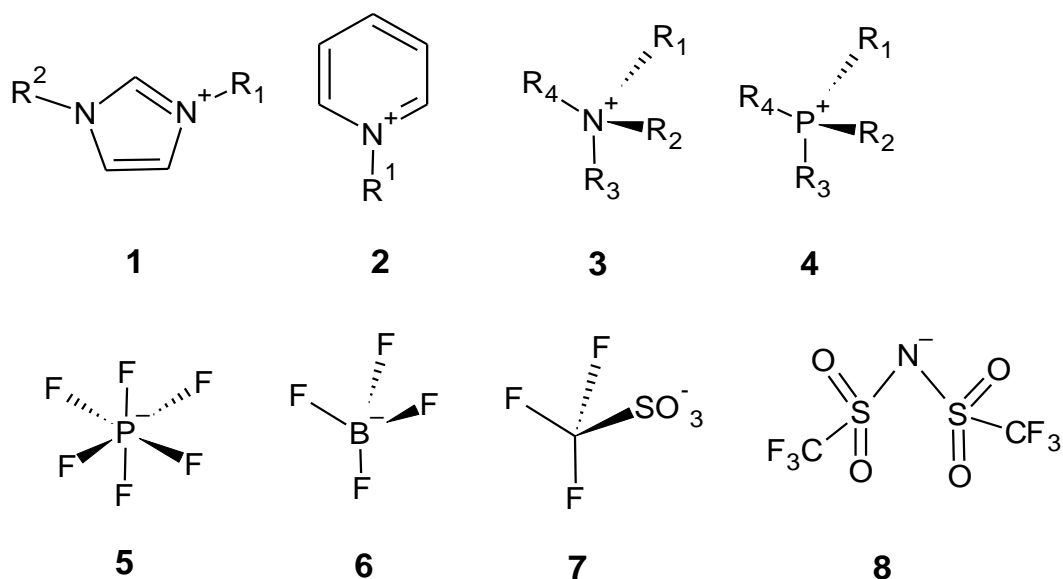


Figure 1-4: Common cations and anions of room-temperature ionic liquids.

Cations: **1.** imidazolium ion; **2.** N-alkyl pyridinium ion; **3.** tetraalkylammonium ion; **4.** tetraalkylphosphonium ion. R1, R2, R3, and R4 are alkyl groups and can be the same or different. Anions: **5.** hexafluorophosphate ([PF6]); **6.** tetrafluoroborate ([BF4]); **7.** trifluoromethylsulfonate ([OTf]); **8.** bis(trifluoromethanesulfonyl)imide ([Tf2N]) [33]

A new subclass of polyelectrolytes known as Polyionic liquids (PILs) have emerged from the incorporation of ionic liquids into polymer chains. PILs uniquely combine the electroconductive and thermally stable properties of ILs and mechanical strength of polymers that enable newer

multifunctional and processing properties, see **Figure 1-5**. Some notable applications of PILs are as thermoresponsive materials, carbon materials, catalysts, separation, adsorption, energy harvesters, storage materials, and bio-related applications [34–37]. In electrochemical applications, ion conductivity of PILs is harnessed in the development of batteries and fuel cells [38,39]. One of the characteristic property of PILs is that their ionic conductivity is typically two orders of magnitude lower than their corresponding IL monomer, because of limited mobility of the polymerized species (cation or anion) [40]. For this reason, PILs are generally considered as single ion conductors. However, when compared to conventional solid state polymer electrolytes, PILs are reported to exhibit higher conductivities (ranging from 10^{-11} to 10^{-5} S cm^{-1}) [41]. There are also reports of PIL/IL blends or ionogels (formed from doping ILs into PILs) demonstrating enhanced performance as conductive materials for ion transport [42].

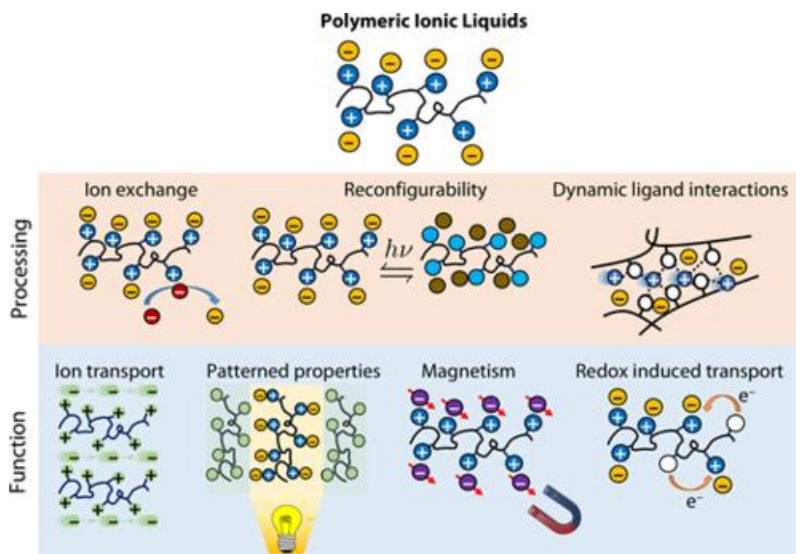


Figure 1-5: Processability and Functional properties of PILs [43].

1.4 Purpose and Significance

Overall, immobilized Resin-Wafer EDI (RW-EDI) holds promising prospects for high energy efficient water desalination than other previously mentioned technologies. Despite its superiority over other desalination technologies, EDI still faces challenges related to specific energy consumption which negatively impact operating costs [18]. Two main factors are responsible for energy performance; operating conditions and material properties (i.e. membranes and resins). While several research studies have focused on investigating optimum operating conditions (such as voltage and flow rate) of EDI systems and developing newer membrane materials, insufficient work has been done on improving resin properties [44–46]. Transport ability of ion exchange resins in EDI module is critically important for effective deionization of water. However, the challenge lies in minimizing the dead zones inherent in the resin bed. Dead zones are formed when the non-conductive binding polymer blocks the active sites of cation and anion resins, impeding the transport of ions, and consequently raising the energy requirements of the system [47]. One possible solution is to establish a continuous path of travel for ions within the bed with as minimal resistance as possible. This can be achieved by utilizing polyelectrolytes, specifically polyionic liquids as a conductive support to the solid resin media.

1.5 Research Objectives

Herein, the purpose of this research is to develop robust resin wafer design with PILs and investigate its impact in desalination of brackish water via EDI. ***The hypothesis is: replacement of conventional elastomeric binders of previous wafer designs with charged polymers will significantly increase ionic conduction in ion exchange resin and improve energy performance of RW-EDI in brackish water desalination.*** To the best knowledge of the author, incorporation

of PIL as an enhancement to the conductive media of RW-EDI systems has not been previously reported. Thus, this research is focused on the following objectives:

- Modify present resin wafer characteristics by replacing conventional binding agents with PIL to create a robust resin wafer.
- Examine changes in ionic conductivity of the PIL functionalized resin wafer.
- Assess the physical properties of modified wafers and its effect on ion removal.
- Investigate the influence of fabricated materials on impaired water desalination in the areas of Removal efficiency (complete ion removal), Current response, Specific energy consumption and Current Efficiency of the EDI process.

CHAPTER 2

2. BACKGROUND/LITERATURE REVIEW

2.1 Scope of This Chapter

In this chapter, a brief overview of early concepts of EDI and progression of the technology are highlighted. The theory governing transport mechanisms and performance in EDI systems is presented. The key parameters for evaluating EDI performance are explained. Then, a review of previous applications of resin wafer technology as it pertains to operational and material developments in EDI is also discussed. The limitation of EDI system is then put in perspective by a critique of the current state-of-the-art technology. Finally, based on this limitation, a potential solution in the form of poly(ionic) liquid is put forward.

2.2 Electrodeionization: Early History and Developments

Paul Kollsman first introduced EDI in 1953. He developed the device for the treatment of ionic mixtures [48,49]. Following this invention, Walters et al. [49] of Argonne National Laboratory applied EDI for the removal of radioactive species from industrial water. In 1959, Glueckauf proposed a theoretical explanation of the ion removal process that enabled a deeper understanding of the EDI process [50]. His work paved the way for other researchers to broaden the knowledge of EDI principles- such as the mechanism of electroregeneration [51–53]. It was not until late 1980 that Continuous Electrodeionization (CEDI) was successfully commercialized by IONPURE for purifying water. Since then, commercial EDI systems have continuously

featured in industrial plants, particularly in power and semiconductor plants, for water purification. To date, investigations into EDI still thrive, aimed at unravelling its potential, creating newer applications and addressing key areas of research interest [18], for example:

- Understanding the mechanisms of ion transport aimed at achieving better energy efficiencies.
- Understanding the interrelationships among the properties of components that make up resin wafer (such as polymer chemistry and ion conductivity).
- Developing methods to balance energy consumption and water recovery to ensure cost effectiveness and large-scale deployment.

2.3 Theoretical Background

2.3.1 Transport in Ion Exchange Membranes

Transport across ion exchange membranes in electro-dialytic systems is driven by both concentration and electrical potential gradients. In solution, salts dissociate into cations and anions. When an electrical potential is applied, the ions travel in opposite directions to their respective electrodes, with each carrying a positive or negative charge. As a result, transport in membranes is typically described as a function of the amount of charge. Thus, the rate of total amount of charge transported across a given area is expressed as:

$$\frac{I}{F} = c^+(u)(+e) + c^-(-v)(-e) = ce(u + v) \quad (2-1)$$

where I is the current in amps and F is the Faraday constant that expressed the charge in terms of current flow in Coulomb per mol. Cation and anion concentrations are designated by c^+ and c^-

respectively. The velocity of cations moving under an external force is u while anion velocity is described as $-v$. The terms $+e$ and $-e$ denote the electronic charges carried by both cations and anions respectively.

2.3.2 Transport in Ion Exchange Media of EDI

At low solution concentrations, the velocity of ions within the dilute chamber of an ED cell slowly retards. When this chamber is filled with resins (as in the EDI cell), conductivity through this solid media exceeds that through the dilute solution by several orders of magnitude (between 1000 and 10,000), because of the high concentration of mobile ions within the resin [25]. The mechanism of ion removal within the in EDI cell was described by Glueckauf as occurring in two stages:

- i. Diffusion of positively charged ions into cation resin and negatively charged ions into anion resin; and
- ii. Ion conduction at the resin/membrane interface.

Since concentration of ions within the resin is higher than the solution, removal of ions is controlled by (i). This ion removal controlling step is dependent on three factors:

- Interface between the solid and the solution.
- Thickness of the liquid layer through which ion diffusion takes place.
- Concentration gradient between the solid and liquid phase.

At the rate limiting step, the applied potential difference causes ions to migrate via the packed resin bed, towards the membranes. Wyllie et al. further developed a model (porous plug) to

describe the conductive patterns of the bed [54]. The model operates on the principle that flow of electrical current follows three different main routes (see **Figure 2-1**):

- Through resins in contact with each other
- Through alternating layers of resins and interstitial solution
- Through the interstitial spaces within the packed bed (i.e. liquid layers)

Therefore, specific conductance of the resin bed which considers all three flow routes, is defined by the following elements;

$$\kappa_b = \kappa_1 + \kappa_2 + \kappa_3 \quad (2-2)$$

$$\kappa_1 = \frac{a\kappa\bar{\kappa}}{d\kappa + e\bar{\kappa}} \quad (2-3)$$

$$\kappa_2 = b\bar{\kappa} \quad (2-4)$$

$$\kappa_3 = c\kappa \quad (2-5)$$

$$a + b + c = 1 \quad (2-6)$$

$$d + e = 1 \quad (2-7)$$

where

κ_b : Specific Conductance of resin bed

κ_1 : Specific Conductance of solid and interstitial solution

κ_2 : Specific Conductance of solid

κ_3 : Specific Conductance of liquid

κ : Specific Conductance of interstitial solution

$\bar{\kappa}$: Specific Conductance of resin

The terms ‘*a*’, ‘*b*’, ‘*c*’, ‘*d*’ and ‘*e*’ are geometric parameters that are representative of the fraction of conductance elements relative to either the solid, solution or solid/interstitial solution

boundaries. These parameters can be determined from the graph of specific conductance of bed vs that of interstitial solution as presented in **Figure 2-2**

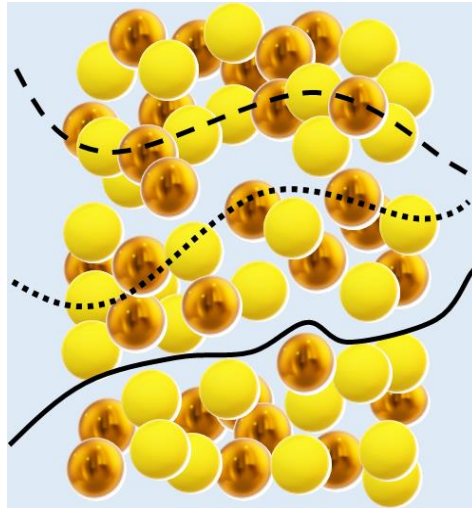


Figure 2-1: Conduction routes in resin bed, reproduced from [25]

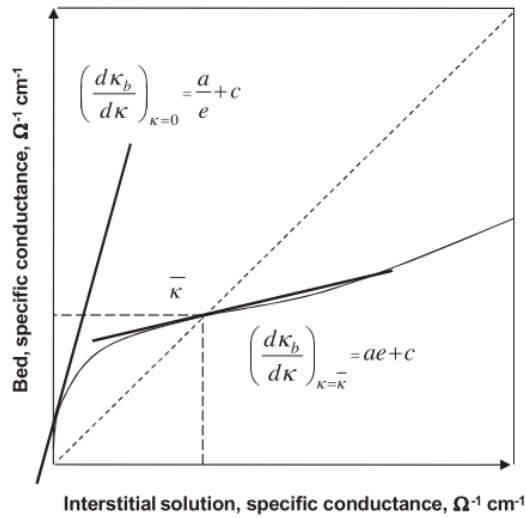


Figure 2-2: Plot of bed specific conductance vs interstitial solution specific conductance, to calculate geometric parameters for the Wyllie model, reproduced from [25]

2.3.3 EDI performance parameters

Evaluating EDI performance is dependent on the analysis of the following key parameters:

I. Removal efficiency (η_r) is a measure of how many ions are removed from the EDI process.

It is defined as:

$$\eta_r(\%) = \frac{(C_i - C_o)}{C_i} \times 100 \quad (2-8)$$

where C_i and C_o are the initial and final ion concentration of feed stream respectively.

Concentration of feed is given as mass concentration in [g/L]

II. Current efficiency (η_c) measures the effective transport of ions across the ion-exchange membranes and wafers for a given applied current.

$$\eta_c(\%) = \frac{z \times V_f \times (C_i - C_o) \times F}{I \times N_{cp} \times MW \times t} \quad (2-9)$$

where z is the valence of ion, V_f is the volume of diluate feed, F represents Faradays constant, I is the average stack current, N_{cp} refers to the number of cell pairs, MW is the molecular weight of ion and t is the total operation time. In EDI systems, current efficiencies greater than 80% are typically desired but may be lower due to the impact of ion exchange material properties.

III. The processing productivity (ϕ) is typically defined as the ratio of the feed processed rate to the total active cross-section membrane area.

$$\phi(Lh^{-1}m^{-2}) = \frac{V_B'}{t'A} \quad (2-10)$$

where V_B' is the feed volume in a batch operated EDI, t' is time to reach the target effluent concentration, and A is the effective membrane area. It should be noted that balancing energy consumption and productivity is critical in order to maximize process economics of EDI systems.

IV. Specific Energy Consumption, SEC: Power consumption (E) of the process is determined by:

$$E [kW] = I^2 \times R \quad (2-11)$$

where R is the electrical resistance of the system.

The SEC is related to electrical energy directly used to produce one unit of purified water or removal of 1 kg of salt. This excludes energy consumed by other process units (i.e. pump). SEC is defined as:

$$SEC [kWh/m^3] = \frac{V \times \int_0^t I dt}{V_f} \quad (2-12)$$

$$SEC [kWh/kg] = \frac{V \times \int_0^t I dt}{(C_i - C_o) \times V_f} \quad (2-13)$$

Where V is the applied voltage to the system.

V. Energy efficiency: relates the minimum work of desalination to the actual energy consumed by the process.

$$\eta_e (\%) = \frac{W_{min}}{W_{actual}} \times 100 \quad (2-14)$$

where W_{min} is the theoretical minimum energy and W_{actual} refers to the actual amount of energy supplied to the system. In principle, the W_{min} is determined from the assumption that desalination occurs as a thermodynamically reversible process and is in fact equal to the free energy of mixing, given by:

$$-d(\Delta G_{mix}) = -RT \ln a_w dn_w = \Pi_s \bar{V}_w dn_w \quad (2-15)$$

where ΔG_{mix} is the free energy of mixing, R is the ideal gas constant, T is the absolute temperature, a_w is the activity of water, n_w is the number of moles water, Π_s represents the osmotic pressure

of saline water, and \bar{V}_w is the molar volume of water [55]. The integration of **equation 2-15** gives the theoretical minimum energy for desalination as a function of feed salinity and recovery ratio i.e. pure water to initial feed water. In **Figure 2-3**, the theoretical minimum energy of desalination for impaired water with salinity of 5 g/L is 0.11 kWh/m³ and 0.23 kWh/m³ at recovery ratios of 50% and 90% [47].

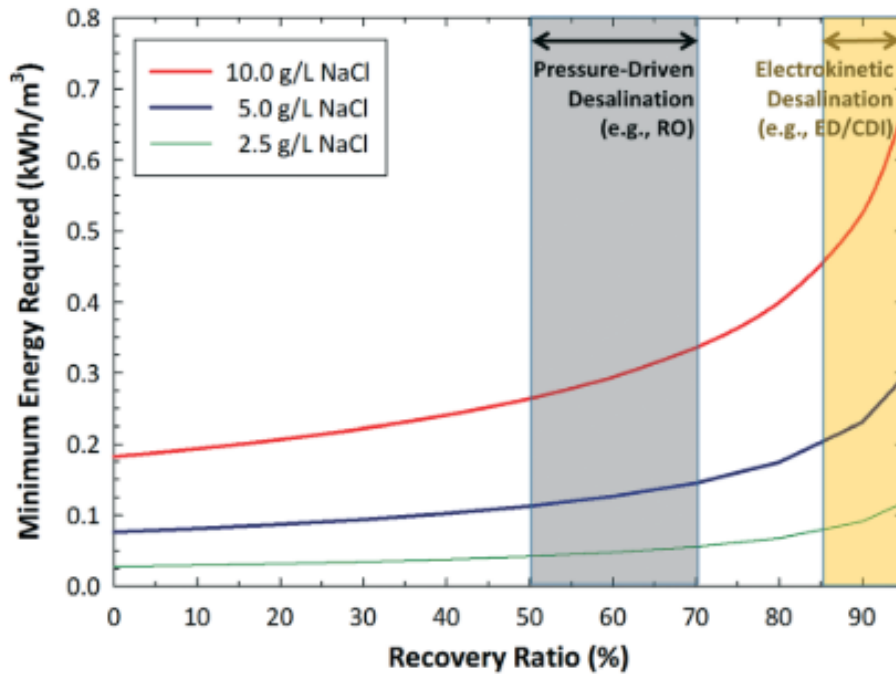


Figure 2-3: Theoretical minimum energy for brackish water desalination as a function of recovery ratio. Reproduced from [18]

2.4 Resin Wafer Technology

Advancements in ion exchange resin development have been targeted at optimizing properties that influence transport i.e. creating a continuous path for ion transfer. Early commercial EDI modules operated as a mixed bed, layered bed, or separate bed resin packed freely in the diluate chambers, however, there were a few limitations with these configurations. Nonuniform displacement of resins, reduction of active sites and escaping of beads were reported as some of

the problems exhibited by packed beds. Another limitation resulting from the resin packing is leakage of ions within compartments leading to a contamination of feed by the concentrate stream. Furthermore, EDI suffered uneven flow distribution within the diluate compartment caused by flow channeling in loosely packed resin beds. To prevent these problems, immobilized ion exchange resins were introduced into the system which served to boost ion transport and separation performance of EDI through improvements in wafer characteristics.

Pioneering work on immobilized resin wafers utilized finely dispersed fluorinated latex and thermoplastic binders (LDPE/HDPE polyethylene) [56]. Further advancement into resin wafers construction aimed to improve the characteristics of ion exchange material and extend EDI application. Lin et al. [57] performed an investigation comparing properties of resin wafers bound by latex and polyethylene integrated with an electrically conductive particle. It was discovered that the latter displayed higher separation efficiency and a 10-fold increase in electrical conductivity than latex-based resin wafer. Additionally, Yeon et al. [58] studied the characterization and feasibility of ion exchange polyurethane as conductive spacers in EDI. In this study, polyurethane based immobilized resins showed good mechanical strength, permeability and a consequent increase in active conducting sites that enhanced cobalt ion removal rate from water. Ho et al. [59] studied wafer compositions and the effects on ion removal. In their research, after varying the resin components, a ratio of 1:1.5:4.6 of polyethylene, sugar (as porogen), and resin respectively was proposed as the optimal formulation for resin wafer fabrication. They concluded that cation-anion resin ratios, polymer volumes and resin selectivity ultimately influenced the removal of ions in the RW-EDI.

Ever since the introduction of wafer technology, researchers have studied how conventional resin wafer impact EDI performance under varying operating conditions in common

applications. For example, Datta et al. [20] tested the efficacy of RW-EDI on the separation of acidic impurities from hydrolysate liquor and pH control of the solution. The results showed that RW-EDI achieved greater than 99% and 95% removal of sulfuric acid and acetic acid from liquor, respectively. Lopez et al. [31] also studied separation of organic acid via wafer-based technology. They reported that application of RW-EDI technique for organic acid recovery resulted in an improvement in the system current efficiency while power consumption fell below 2 kWh/kg. In more recent studies, Pan et al. [47] evaluated the effect of operational parameters on key performance indicators of conventional RW-EDI desalination of impaired water. They found the specific energy consumption to be 0.35-0.66 kWh/m³ with a productivity of 20.1– 41.3 L h⁻¹ m⁻², indicating that EDI can be successfully applied for energy efficient impaired water reclamation. It was also reported that the dead zones (caused by the binding polymer) minimized total achievable energy consumption. Further energy savings is still desired to enable deployment of RW-EDI technologies on a large scale [18]. Thus, it has become necessary to develop novel materials that could aid reduction in energy demands of EDI while maintaining optimal separation performance of the process.

2.5 Poly(ionic liquid)s as novel materials for ionic conductivity in RW-EDI

In RW-EDI, ionic conductivity of the bed plays a crucial role in energy consumption of the system. Conduction via bead-to-bead contact in **Figure 2-4** represents the most efficient pathway for current in EDI. Transfer of ions must occur between resins of the same type (i.e. anion to anion) and follow a continuous path towards the electrode. If the pathway is interrupted (i.e. discontinuous resins), ions are displaced into the surrounding solution and subsequently picked up by neighboring resin bead of similar type. Consequently, the erratic movement of ion within the bed

raises the electrical power needed for ion transfer and reduces the cell efficiency. Additional contact resistance is created as the polymer used in the immobilization of resins hinders the smooth transmission of ions. This resistance is depicted in the equivalent circuits of **Figure 2.5** for conventional EDI (**Figure 2.5(a)**) and RW-EDI in (**Figure 2-5(b)**)

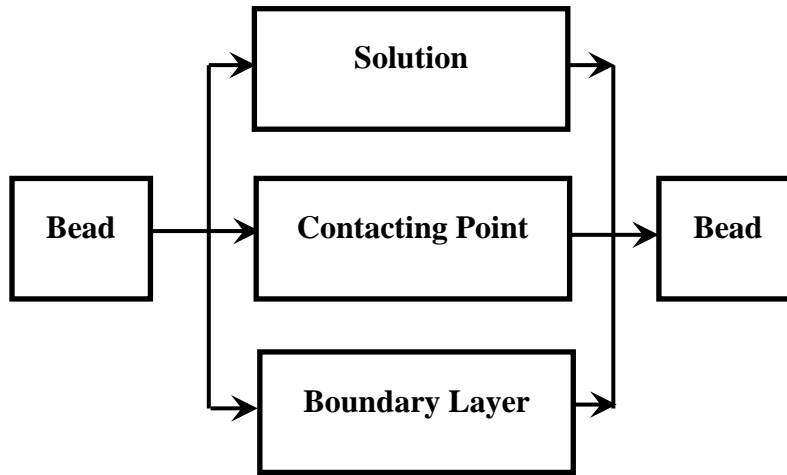


Figure 2-4: Schematic representation of the paths that the current may take [59]

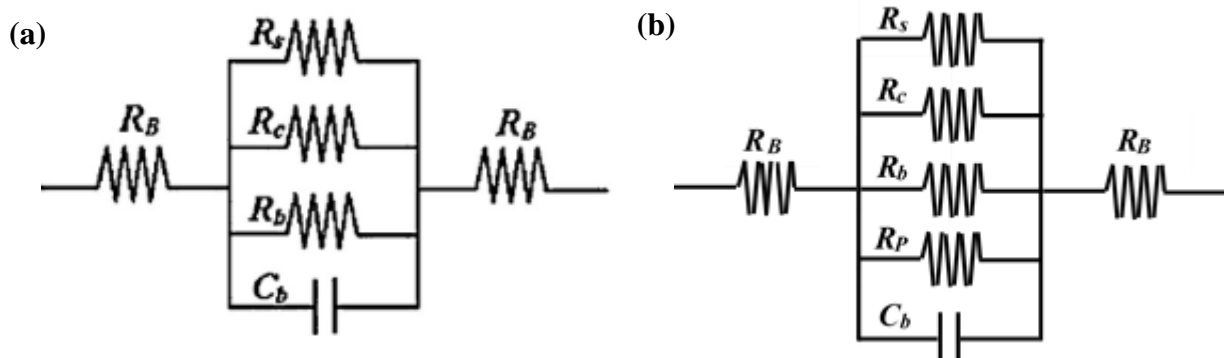


Figure 2-5: (a) Equivalent circuit for determining the special dispersion of current in conventional EDI. (R_B is resistance of the bead, R_c is resistance of the contacting point, R_s is resistance of the solution, R_b is resistance of the boundary layer, and C_b capacitance of the boundary layer [24]. (b) Equivalent circuit for determining the special dispersion of current in RW-EDI. (R_B is resistance of the bead, R_c is resistance of the contacting point, R_s is resistance of the solution, R_b is resistance of the boundary layer, R_p is the resistance of the polymer and C_b capacitance of the boundary layer). Modified from [24]

It can be suggested that the presence of the polymer (which is polyethylene in most resin wafers) contributes to the overall resistance of the bed, hence the low energy efficiency of the stack. The use of better conducting materials is therefore needed. In a bid to enhance wafer characteristics and performance in EDI processes, polymer ionic liquids (PILs) have been identified as substitutes to conventional binding materials. This is because they uniquely combine the electroconductive and thermally stable properties of ILs and the mechanical strength of polymers. This has created opportunities in electrochemistry with more potential applications yet to be explored. Some of the relevant properties have been reported in recent studies. In fuel cell applications, PIL-based membranes are highly desirable strategies for clean energy production. Such polymer electrolyte membranes (PEM) have been synthesized by Yan et al. where PILs and silica particles were incorporated into proton conducting membranes [60]. The resultant membranes possessed good flexible, mechanical properties and thermal stability. They also attributed the significantly high proton conduction obtained to the ion transport channels/network structures formed in the membranes. In electrochemical device applications, Ambrogi et al. [61] reported that thiazolium PIL-based binder showed superior charge mobility of ion in lithium batteries over Poly(vinylidene difluoride) (PVDF) based binders. They further concluded that other types of PIL (imidazolium, phosphonium, and guanidinium) could be effectively applied as binders in electrochemical devices. The impact of phosphonium-based (i.e. P-based) PILs as conductive materials has been on the up rise in recent research studies [62]. This is because they exhibit favorable stability and conductivity compared with their imidazolium-based (i.e. N-based) counterparts. While P-based PILs show compelling potential as solid state polyelectrolytes, they have mostly served as ion exchange materials than as electrolytes [63]. P-based ILs recently featured in Polymer Inclusion Membranes (PIMs) to serve as ion carriers and facilitate the

transport of ions from aqueous chloride solutions, suggesting its usefulness in liquid separations systems [64].

Considering all the benefits addressed above, no prior study exists on the use of PILs in electrokinetic applications, including in aqueous media. Resin wafer formulation integrating PILs can aid ion transport and improve the electrokinetic performance of EDI technology while maintaining the mechanical integrity of the wafer. Ions can travel from resin to resin via the polymer because of the characteristic crystal defects and high density of charge carriers in PILs, which influence conductivity. This can be observed by an increase in the current response of RW-EDI system, which is the result of enhanced speed of ions that traverse the resin bed.

CHAPTER 3

3. EXPERIMENTAL MATERIALS AND METHODS

3.1 Materials and Instrumentation

Trioctylphosphine (97%), 4-vinylbenzylchloride (90%), Bis(trifluoromethane)sulfonimide lithium salt and 2-Hydroxy-2-methylpropiophenone used for the preparation of phosphonium IL/PIL were obtained from Sigma Aldrich and 3M. Amberlite IRA-400 chloride, Amberlite IR120 (hydrogen form) and Polyethylene (Ultra-high molecular weight) used during wafer fabrication were also obtained from Sigma Aldrich. Sucrose and Sodium chloride (used as porogen) were obtained from VWR. Properties of ion exchange resins are detailed in **Table 3-1**. Membranes used in EDI were NEOSEPTA AMX and CMX purchased from Tokuyama America. ¹H Nuclear Magnetic Resonance (¹H NMR) with CDCl₃ as solvent were performed on AV 400 MHz (Bruker Avance III HDTM NMR spectrometer). Fourier Transform Infrared Spectroscopy (FTIR) was conducted at room temperature using an Agilent Technologies Cary 630 FTIR spectrometer in attenuated total reflectance (ATR) mode. Surface characterization of resin wafer was examined via OMAX A35100U Digital USB Microscope Camera. Images of small wafer samples were obtained to confirm that conducting sites of resins were not completely hampered by the binding polymer. The ionic conductivity/resistance of the wafers was measured by Electrochemical Impedance Spectroscopy (EIS) using Princeton Advanced Research EG&G 263A

and the resistance calculated from the Nyquist plots. Ionic concentrations of the feed solutions were measured with a Traceable conductivity probe from Fisher Scientific.

Table 3-1: Detailed Specification of Ion Exchange Resins

	Cation Exchange Resin	Anion Exchange Resin
Type	Amberlite® IR120 hydrogen form	Amberlite® IRA-400 chloride form
Matrix	Styrene-divinylbenzene	Styrene-divinylbenzene
Matrix active group	Sulfonic acid	Quaternary Ammonium functional group
Cross-linkage	8%	8%
Moisture	53-58%	40-47%
Particle size	620-830 μm	600-750 μm
Operating pH	0-14	0-14
Capacity	1.8 meq/mL by wetted volume	1.4 meq/mL by wetted volume

3.2 Synthesis of Ionic Liquid monomer

The polymer functionalized ionic liquid employed in the modified wafer was synthesized from phosphonium-based IL known as Trioctyl(4-vinylbenzyl)phosphonium-bis(trifluoromethane)sulfonimide i.e. [P888(4-VB)][Tf₂N], as illustrated in **Figure 3-1**.

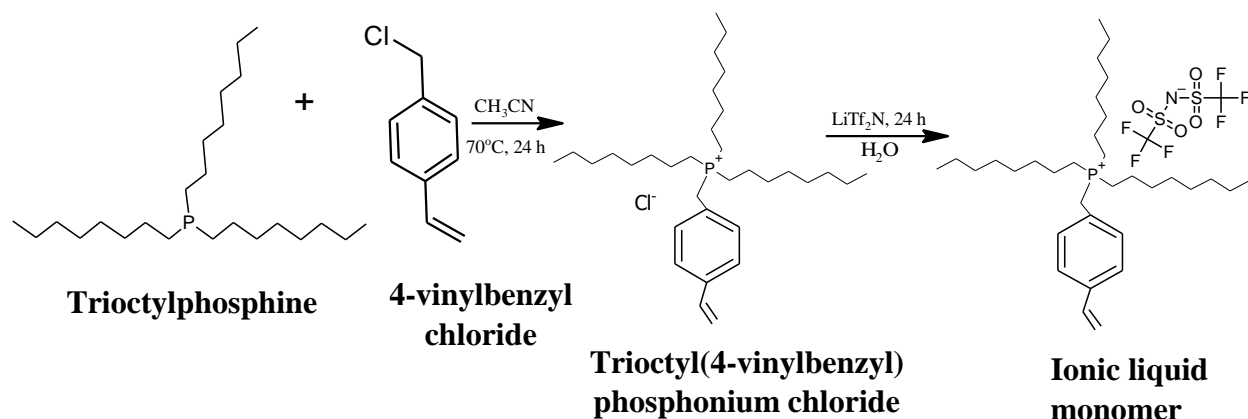


Figure 3-1: Synthesis of Trioctyl(4-vinylbenzyl)phosphonium-bis(trifluoromethane)-sulfonimide i.e. [P888_(4-VB)][Tf₂N]

The IL was synthesized in accordance with Barsanti et al. [65], although slight modifications were made to the procedure. Under an argon atmosphere, trioctylphosphine (19.94 g, 53 mmol) was added to 30mL of acetonitrile in a double neck round bottom flask. An equimolar amount of 4-vinylbenzyl chloride (8.12 g) was added to the mixture, heated to 70 °C and allowed to stir for 24 h. The resulting mixture was washed with diethyl ether and all solvents were removed via a rotovap. The mixture was dried under schlenk line for 24 h, resulting in a white solid product- Trioctyl(4-vinylbenzyl)phosphonium chloride ([P_{888(4-VB)}]Cl, 41 g, 84 mmol). The product was dissolved in 100mL of water and anion exchange was carried out with 1.1 molar excess 26.5 g (92.4 mmol) of Li(Tf₂N). The aqueous solution was then stirred for 48 h at room temperature. After the reaction was over, the product was extracted into 100mL dichloromethane and washed five times with 100mL water (or until a silver nitrate test of the product showed no detectible presence of halide). The organic product was then dried over anhydrous magnesium sulfate (MgSO₄) and filtered before removing the solvent via rotovap. Finally, the clear pale-yellow oil product was further dried under schlenk line for 24 h at room temperature until vacuum pressure reached 60 mtorr.

3.3 Wafer Composition and Fabrication

Both conventional-style and modified resin wafers were fabricated using a blend of anion exchange resin beads, cation exchange resin beads. Conventional wafers (PE-RW) comprised of AEX and CEX resins, porogen (Sodium chloride was used in this method because sucrose melted when heated to the desired temperature) and polymer (Polyethene) in a 23:23:15:10 g ratio, respectively. The constituents were uniformly combined and cast into a custom-made PTFE mold until uniform thickness was achieved. Once formed in the mold, the combined mixture was placed in an oven and heated to 146 °C for 3 hours. After heating, the wafer was cooled via ambient air to allow the polymer to set.

Modified wafers (PIL-RW) were fabricated following a slightly different method. Whereas polyethene was used as binding polymer in conventional wafers, PIL-RW were immobilized using PIL [P_{888(4-VB)}][Tf₂N]. Two different formulae consisting of 10:10:6:2.5 g and 10:10:6.5:3 g of anion resin, cation resin, sugar, and IL respectively were considered. Resin/PIL ratio was varied in PIL-RW in order to investigate the effects that each had on wafer's stability and EDI performance.

3.3.1 Solvent Casting Polymer blend

Phosphonium IL was first polymerized with photo initiator (2-Hydroxy-2-methylpropiophenone) under UV light for 3 hours. After photocuring, polymer was dissolved in dichloromethane and stirred continuously until a viscous polymer solution was obtained. The solution was uniformly combined with dry resin constituents, cast onto a mold and then solvent was allowed to evaporate for 15 hours. The resulting wafer was soaked in deionized water to remove any remaining sucrose.

Both PE-RW and PIL-RW were then cut to size to fit the spacer opening of the EDI stack. The average thickness of wafer was 2.5 mm (measured with a micrometer caliper) and each had a cross-sectional area of 12.5 cm².

3.4 EDI Set-Up

Electrodeionization experiments were performed using a Micro Flow Cell (ElectroCell North America, Inc.) setup with ion exchange membranes, PTFE spacers, gaskets, and titanium electrodes as shown in **Figures 3-2** and **3-3**. The EDI stack consisted of diluate, concentrate and rinse compartments separated by alternating spacers and gaskets which permit or hinder flow of feed streams within the stack. The solution of interest was fed into the system (using MasterFlex L/S 77200-62 peristaltic pumps) via two sets of inlet and outlet holes on either side of the EDI cell. The feed stream was channeled to the different chambers through spacers- which included an enclosure for ion exchange wafers (diluate chamber) and turbulence mesh (concentrate chamber). The electrodes were connected to GW INSTRON GPS-3030DD power source used to supply DC power to the system.

Figure 3-4 is an illustration of the electrodeionization system showing the typical arrangement of component parts. The arrows indicate the path for the movement of solution through the compartments, with feed stream flowing in through the inlet ports, circulating through each compartment and leaving upwards through the outlet ports. The rinse compartments are isolated from the diluate and concentrate compartments using closed gaskets. Cross mixing of diluate and concentrate streams is prevented by alternating the spacers, only permitting diffusion of ions through the respective membranes.

Table 3-2: EDI experiment set-up

EDI Set-Up	
Operation Mode	Batch
Diluate & Concentrate Feed Type	NaCl (5 g/L)
Diluate & Concentrate Volume	500 mL
Rinse Feed Type	Na ₂ SO ₄ (20g/L)
Rinse Volume	1000 mL
Number of Cell Pairs	2
Flowrate	150 mL/min
Applied Voltage	PE-EDI vs PIL-EDI (3.0 g IL): 6.5 V & 8 V PE-EDI vs PIL-EDI (2.5 g IL): 6V & 7V
Average operation time	6-9hrs



Figure 3-2: Front view of ElectroCell system showing inlet and outlet ports



Figure 3-3: Side view

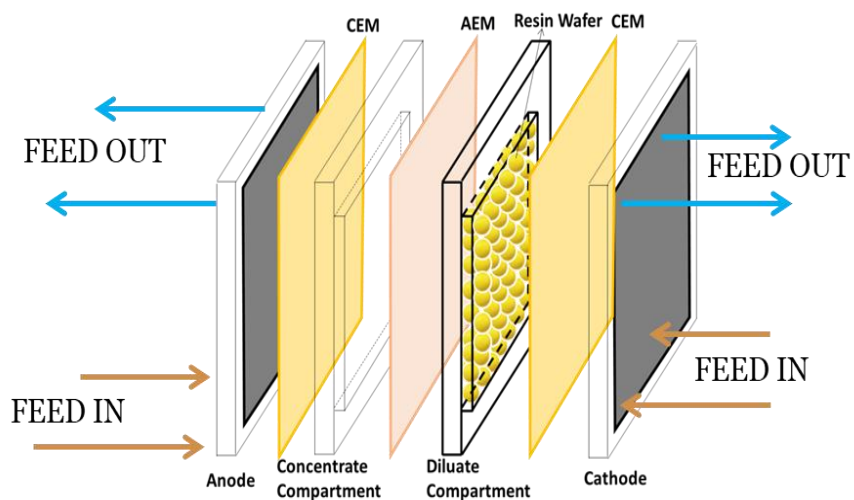


Figure 3-2: Configuration of a Resin Wafer Electrodeionization cell

Sodium chloride (NaCl) solution was used to simulate brackish water for the desalination experiment. Diluate and concentrate chambers were fed with 500 mL of a 0.5 weight % sodium chloride solution, while the rinse chambers contained 1000 mL of 2 weight % sodium sulfate (Na_2SO_4) solution. All experiments were conducted in batch mode for 2 membrane cell pairs at 150mL/min flow rate and varying voltage conditions. In each experiment, voltage was kept constant until current reading reached or fell below 0.02 Amps, indicating a decrease in the population/velocity of ions present in the solution. On average, each experiment ran for 6-9 hours depending on the operating conditions while conductivity readings were taken at hour-long intervals. At the end of each run, the system was washed out with deionized water for twenty minutes. Internal leakage within the system was maintained below 7mL/hr. Above this volume, experiments needed to be repeated. A summary of EDI experimental set-up is highlighted in **Table 3-2**.

The diluate, concentrate and rinse conductivity readings were recorded alongside the current readings at intervals. All experimental runs were repeated three times for accuracy and an average was taken for further calculation of key parameters. Removal Efficiency, Current Efficiency, Specific Energy consumption were all calculated from the resulting data of both PE-EDI and PIL-EDI experiments.

CHAPTER 4

4. RESULTS AND DISCUSSION

4.1 Fourier Transform Infrared Spectroscopy

Synthesizing a polymer with high mechanical stability was essential in the development of a resin wafer with good structural properties. Fourier Transform Infrared Spectroscopy (FTIR) was employed to evaluate the curing degree of the IL monomer and confirm the mechanical properties of PIL. The phosphonium IL was evaluated by analyzing the vinyl (C=C) peak of interest from the 898-933 cm^{-1} band as shown in **Figure 4-1**. The transmittance band at 1152-1213 cm^{-1} was taken as reference peak to estimate the conversion of the vinyl group. The integral of the IL and PIL spectra were used to calculate the degree of polymerization using **Equation 4-1**. The polymerization degree was found to be approximately 89%, indicating high mechanical strength and ability to provide good structural support for the resin bed.

$$\text{Degree of Polymerization (\%)} = \frac{\left(\frac{\text{Area of vinyl peak}}{\text{Area of reference peak}}\right)_{IL}}{\left(\frac{\text{Area of vinyl peak}}{\text{Area of reference peak}}\right)_{PIL}} \quad (4-1)$$

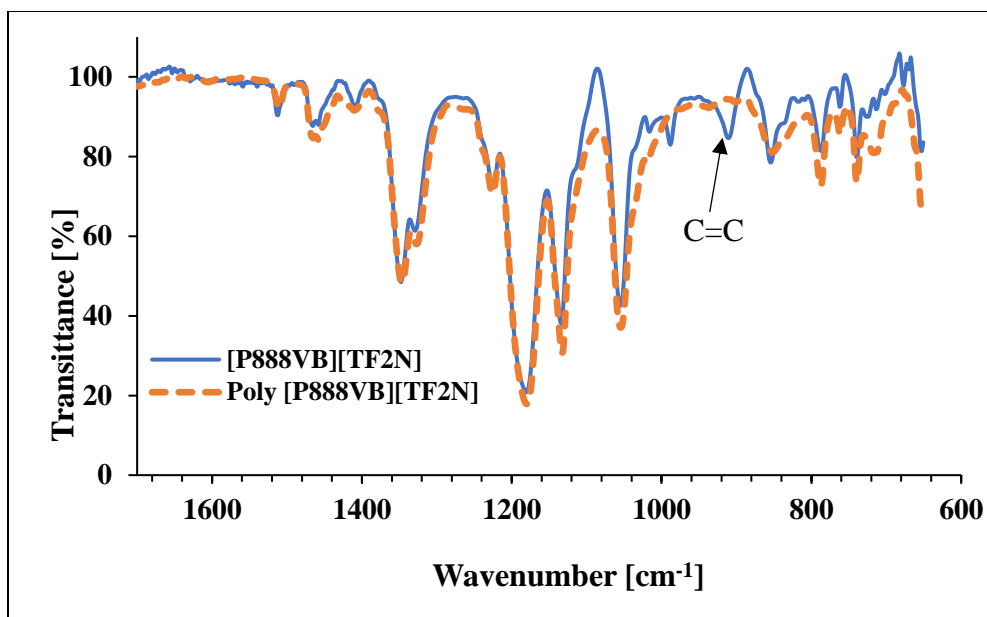


Figure 4-1: IR spectra of IL [P888VB][TF2N] and PIL Poly[P888VB][TF2N]. The change in C=C stretch at 898-933 cm^{-1} of the polymer shows the degree of polymerization (89% approx..)

4.2 Characterization of Resin Wafer as Ion Conducting Spacers

4.2.1 Effect of electrochemical properties of polymer on resin wafer conductivity

Electrochemical Impedance Spectroscopy was conducted to investigate the ionic conductivity of the bed. The impedance measurements were obtained by applying a 100mV AC amplitude and a frequency scan of 1.0 MHz to 1.0 Hz at an initial voltage reading of -0.013V. The resistance was determined from the Z' axis of the Nyquist plot. Ion conductivity was calculated from the **equation 4-1** below

$$\sigma = \frac{L}{AR} \quad (4-1)$$

where σ is conductivity in S/cm, L is wafer thickness in cm, A is the effective area in cm^2 and R is the resistance [Ω]. The bulk conductivity of PE-RW and PIL-RW were $8.64 \times 10^{-6} \text{ Scm}^{-1}$ $2.21 \times 10^{-5} \text{ Scm}^{-1}$ respectively, indicating a one order magnitude increase of ion conductivity in PIL-RW as compared to PE-RW.

4.2.2 Effect of polymer on the morphology of resin wafer

The formulation of PE-RW and PIL-RW greatly influenced the mechanical stability of the wafer. The bulk PE-RW had a more compact packing and a higher degree of mechanical stability before and after soaking in water than both PIL-RW variants, because of the optimal polymer to resin ratio, which had been predetermined in [66]. An examination of the morphology of PE-RW in **“1a & 1b” of Figure 4-2** showed clusters of polyethylene partially enclosing beads, which are thought to hinder the beads from contacting the solution. In the preparation of PIL-RW, using 3.0 g of PIL seemed to induce adequate mechanical support in the wafer. However, this amount of PIL caused a high degree of coating of the resin surfaces as seen in images **“2a & 2b” of Figure 4-2**, that restricted the active sites for ion transport. By reducing the amount of PIL in the wafer to 2.5 g, the resin surface area available for ion transport was slightly maximized as seen in **“3a & 3b” of Figure 4-2**. Both PIL-RW variants appeared to have relatively compact packing density when dry but became structurally weak after soaking in water due to the swelling properties of the PIL. As expected, PIL-RW consisting 2.5 g PIL possessed less mechanical strength than that with 3g PIL, partly due to the insufficient polymer/resin ratio. Nevertheless, the PIL film seemed to form a non-uniform but widespread coating within the bed, which indicated that a continuous pathway for current flow was being created in the PIL-RW.

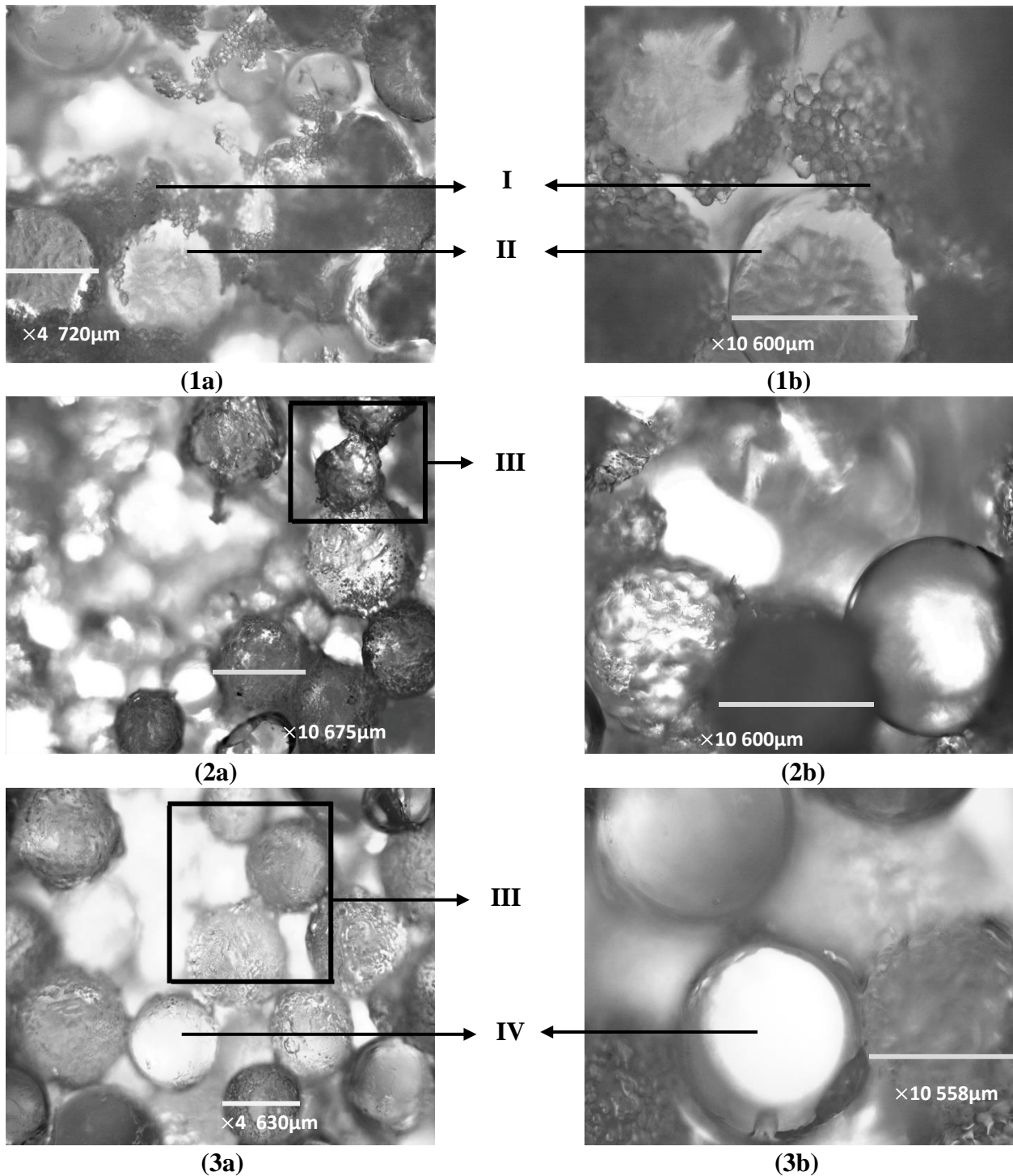


Figure 4-2: Microscope images of PE-RW (1a & 1b), PIL-RW with 3g PIL (2a & 2b) & PIL-RW with 2.5g PIL (3a & 3b) at $\times 4$ and $\times 10$ magnification. I & IV are ion exchange resins, II are Polyethylene clusters around resin beads and III shows two resin beads bound by PIL film.

4.3 Application in EDI system

4.3.1 Effect on Stack Current, Removal Efficiency, and Specific Energy Consumption

In this study, a comparison of the effect of PE-RW and PIL-RW on current and removal efficiency was evaluated for different applied voltages of 6.5V and 7.0V. The results (in **Figure 4-3**) show that when PIL-RW with 3.0 g PIL was used in the system (i.e. PIL-EDI), there was a significant difference in the initial current response across the stack, compared with PE-based EDI (PE-EDI). The reason for the limited cross current can be attributed to the increased resistance that had developed from the obstruction of the resin surface area by the PIL coating. Generally, the incorporation of PIL is expected to facilitate ion movement between resin beads by occupying the alternating layers of the beads and interstitial solution of the porous bed. However, at high PIL to resin ratios, a decrease in the bead to bead interfaces (i.e. main conduction channel) occurs thus, minimizing the pathway for ions to travel. Additionally, the removal rate of ions by PIL-EDI decreases in contrast with PE-EDI for both instances of applied voltage, as shown in **Figure 4-4**. This is also the result of resin surface blockage in PIL-RW that slows down the salt removal process.

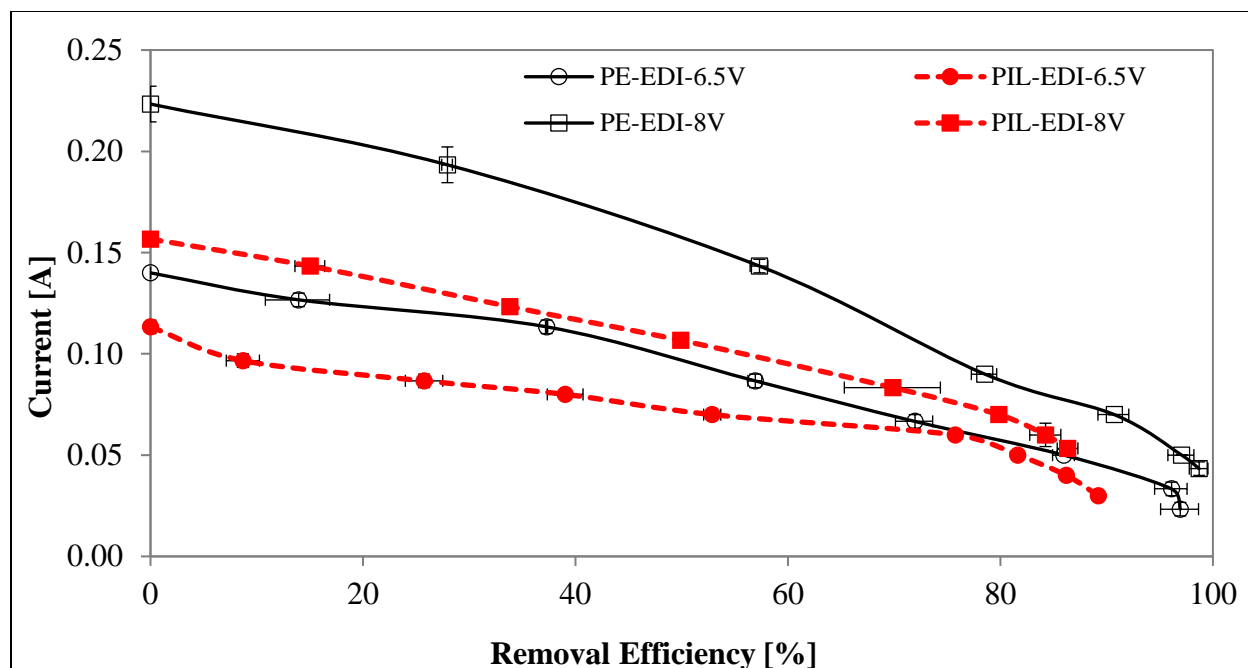


Figure 4-3: Comparisons in average current response and corresponding average removal efficiency of PE-EDI and PIL-EDI (comprising 3.0 g PIL) runs, at 6.5V & 8V.

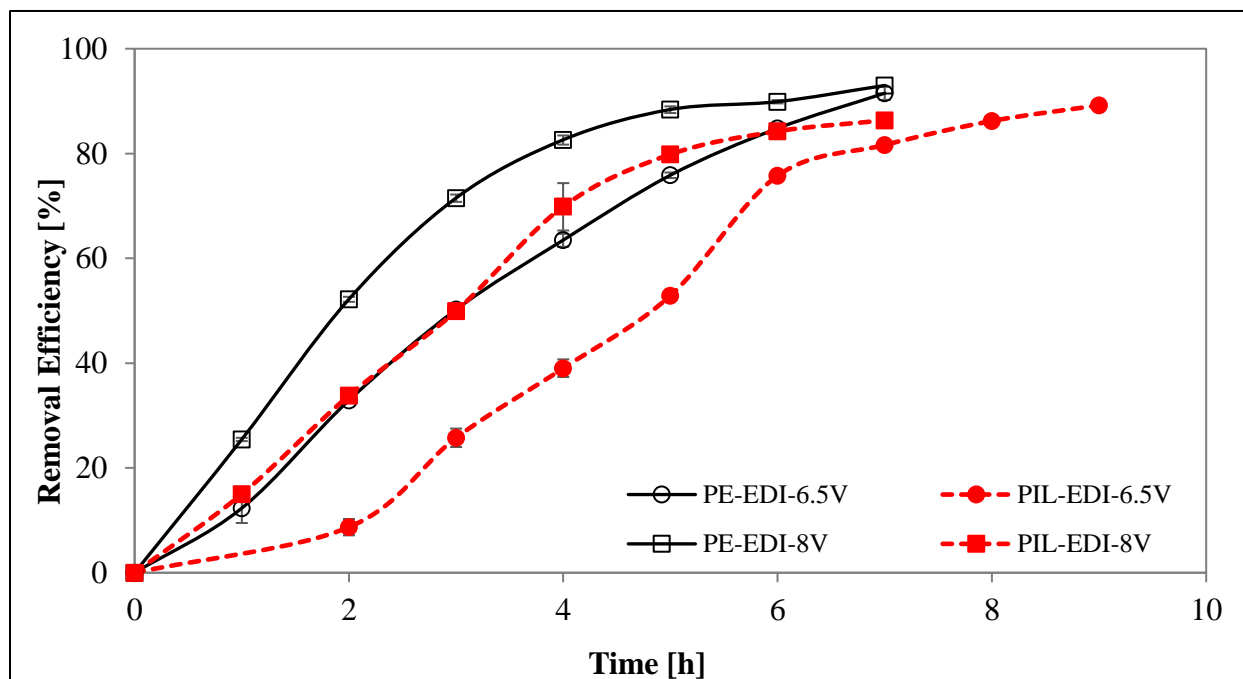


Figure 4-4: Comparing the average removal rate of PE-EDI and PIL-EDI (comprising 3.0 g PIL) runs, at 6.5V and 8V.

Conversely, reducing the PIL/resin ratio (from 3.0g PIL to 2.5g PIL) increases the PIL-RW ability to enhance transport in EDI. This is observed as an increase in the initial current responses of the PIL-EDI compared with PE-EDI, as seen in **Figure 4-5**. Also, at both applied voltages of 6V and 7V, higher current readings were noticed in PIL-EDI than PE-EDI as solution concentration decreased. Furthermore, while both systems reached equilibrium at the same time for both applied voltages of 6V and 7V, a slightly higher removal rate is observed with PIL-EDI stack than with the PE-EDI in **Figure 4-6**.

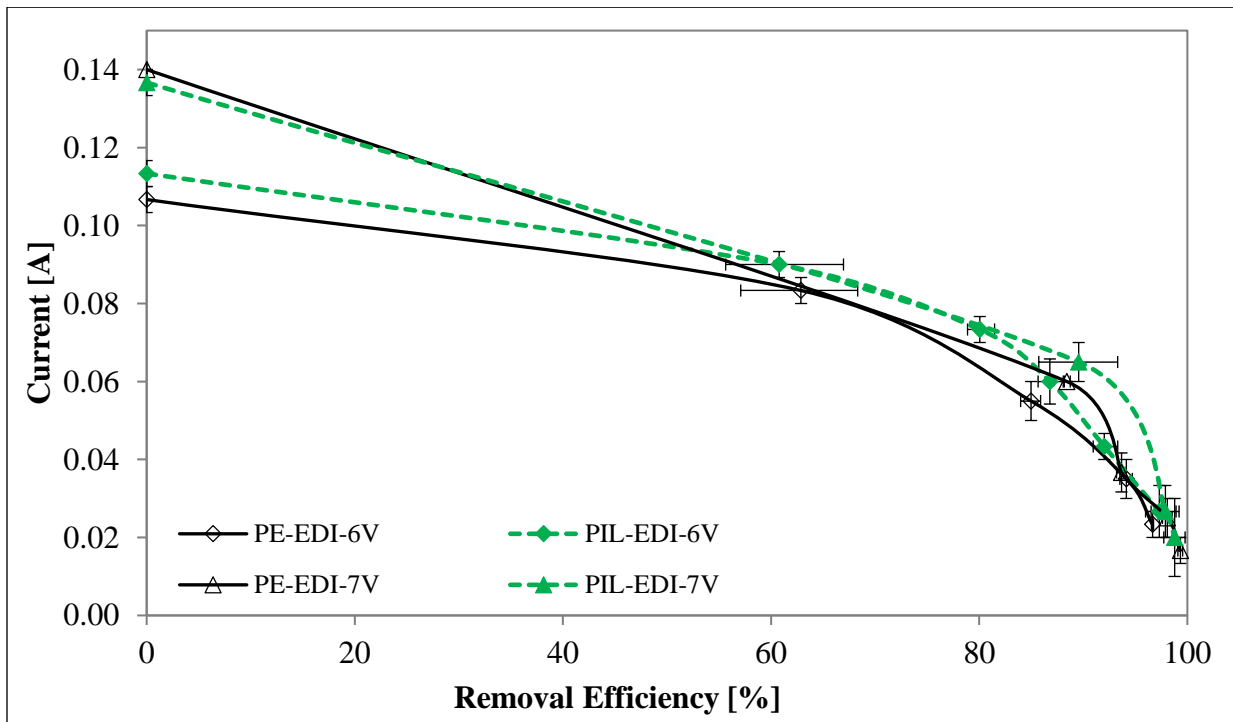


Figure 4-5: Comparisons in average current response and the corresponding average removal efficiency of PE-EDI and PIL-EDI (comprising 2.5 g PIL) runs, at 6 V & 7V.

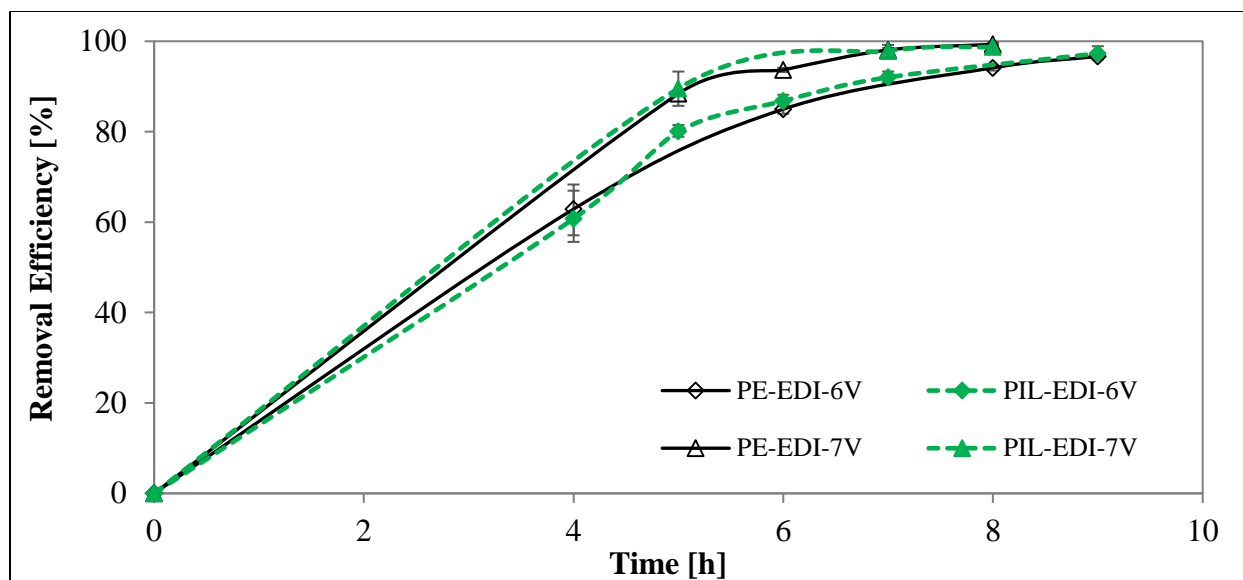


Figure 4-6: Comparing the average removal rate of PE-EDI and PIL-EDI (comprising 2.5 g PIL) runs, at 6 V and 7 V.

4.3.2 Effect on Specific Energy Consumption of system

An analysis of the removal efficiency and specific power consumption is shown for PE-EDI and PIL-EDI (comprising 3.0 g PIL) in **Figures 4-7** and **4-8**, as well as for PE-EDI and PIL-EDI (comprising 2.5 g PIL) in **Figure 4-9** and **4-10**. Generally, specific energy consumption increases with applied voltage, suggesting that voltage should be maintained at an optimal minimum. In all experimental runs, the SEC appears to be lower in PIL-EDI than conventional PE-EDI. As SEC is related to the total ions removed, it was difficult to compare the performances of both PE-EDI and PIL-EDI (comprising **3.0 g PIL**) runs, because removal efficiencies of the latter were generally less than the former. However, characteristic differences in PE-EDI and PIL-EDI (comprising **2.5g PIL**) performance were more noticeable in **Figure 4-9** and **4-10**. This is because at relatively similar removal efficiencies, the latter displayed a lower SEC than the PE-EDI. The only exception

was the second run of PIL-EDI (2.5g PIL) in **Figure 4-9**, which could be related to anomalies associated with the EDI system.

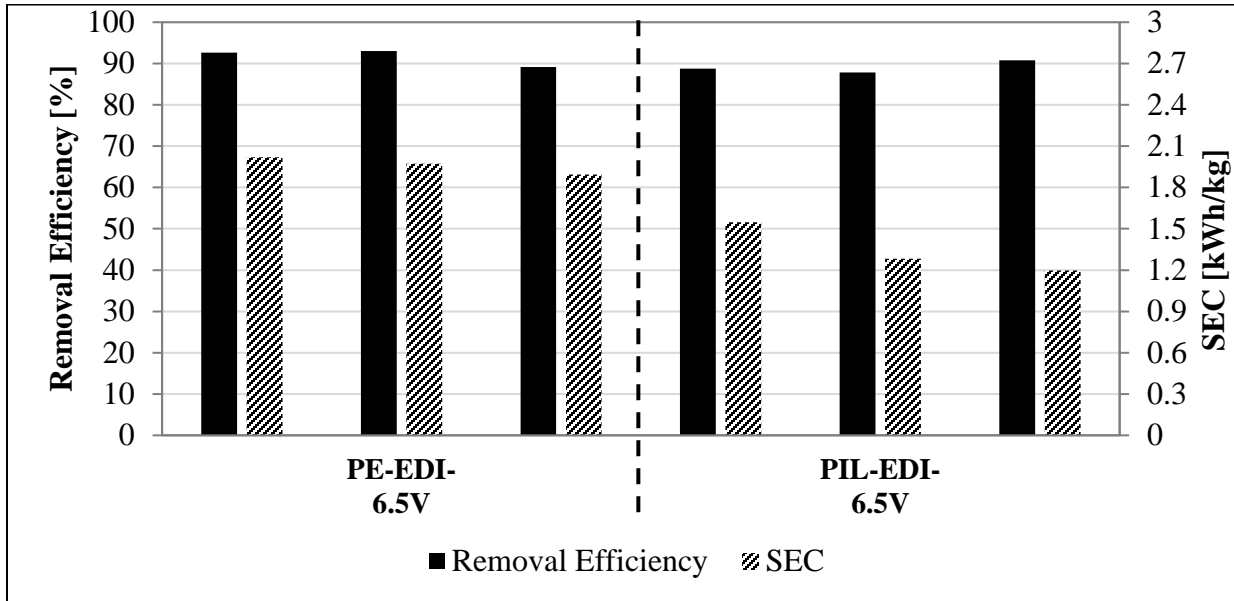


Figure 4-7: A comparison of the removal efficiency and SEC at 6.5 V for PE-EDI and PIL-EDI (comprised of 3.0 g PIL) runs.

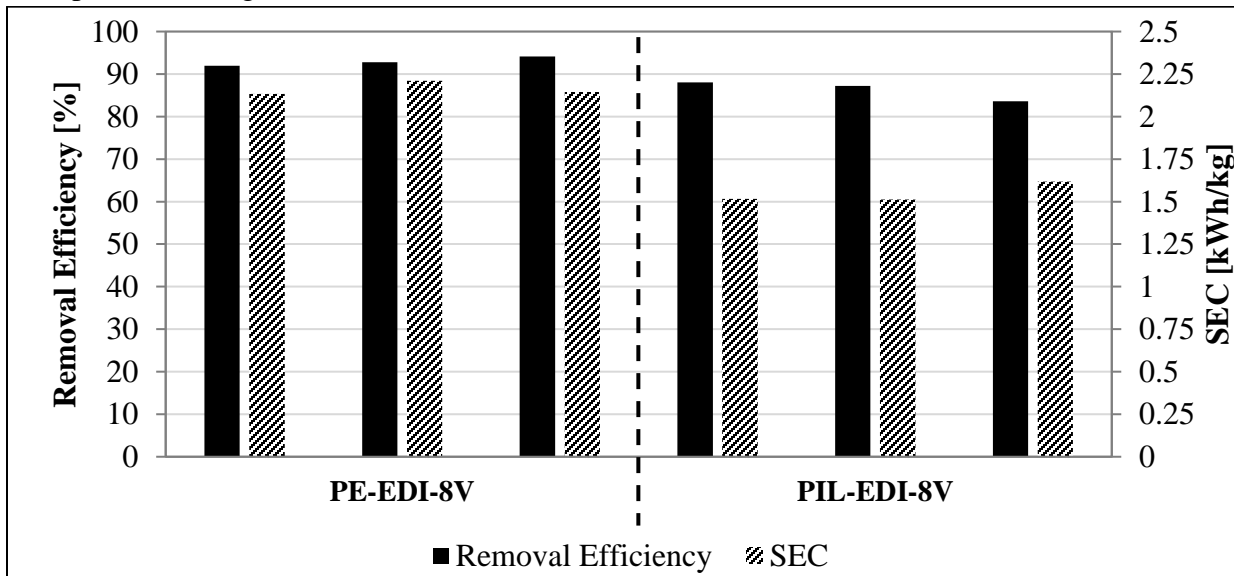


Figure 4-8: A comparison of the removal efficiency and SEC at 8 V for PE-EDI and PIL-EDI (comprised of 3.0 g PIL) runs.

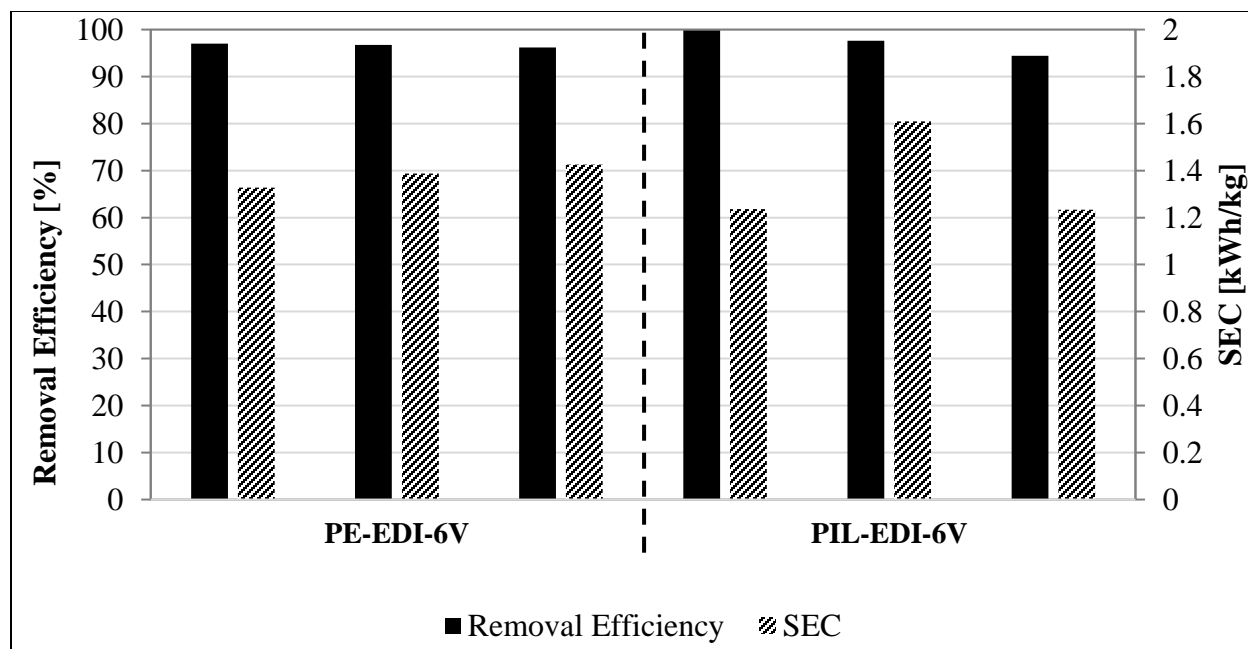


Figure 4-9: A comparison of the removal efficiency and SEC at 6 V for PE-EDI and PIL-EDI (comprised of 2.5 g PIL) runs.

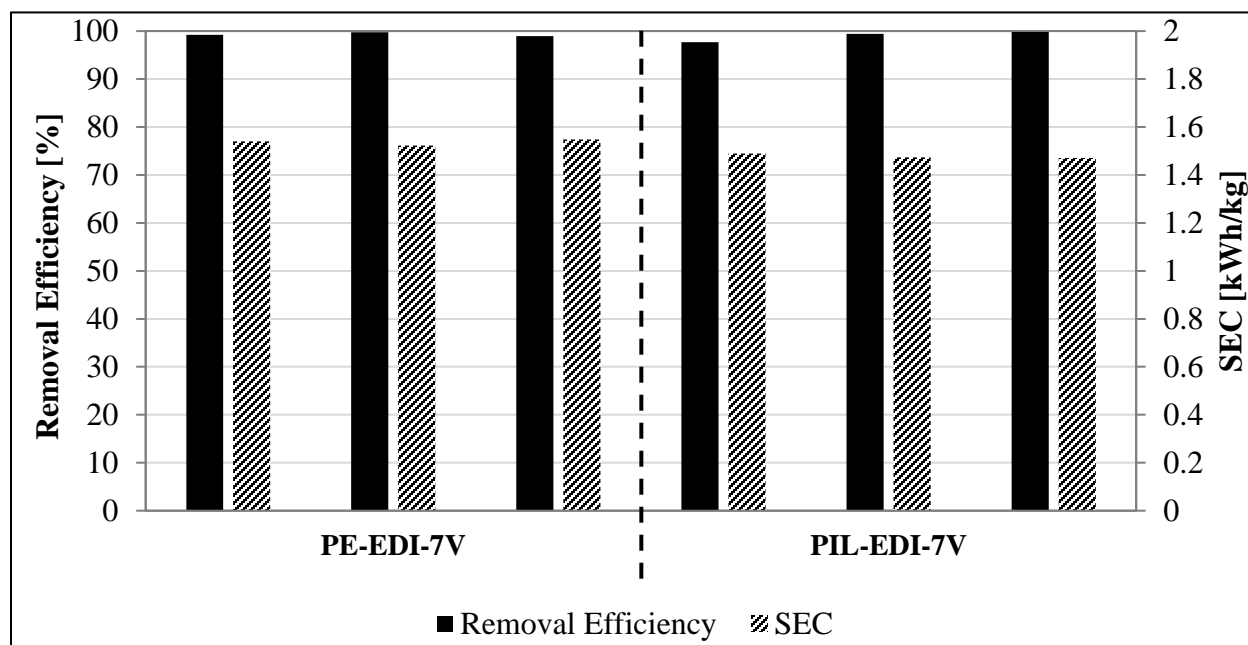


Figure 4-10: A comparison of the removal efficiency and SEC at 7 V for PE-EDI and PIL-EDI (comprised of 2.5 g PIL) runs.

For the lab scale two cell pair EDI configuration, operating at an applied voltage of 6V is ideal because it produced the best removal efficiency and low SEC for both PE-EDI and PIL-EDI systems.

Overall, the SEC data suggests that PIL-RW (2.5 g PIL) generally lowers energy consumption in EDI in comparison to PE-RW. The average reduction in SEC by PIL-EDI (2.5g PIL) across all three runs, were approximately 5% for applied voltages of 6 V and 7 V. This indicates that PIL functionalized wafers enhanced ion transport in EDI, but to a certain degree, as observed in the data analysis above. PIL conductivity and resin formula are some of the factors that limited the scale of improvement in EDI. Ion conductivity in PIL is dependent on the mobility of ionic moieties within the polymer chains. The higher the degree of cure in PIL, the higher the glass transition temperature i.e. T_g . However, to achieve high ion conductivities, lower T_g is necessary as more mobile matrices are available for free movement of counterions. Therefore, balancing the degree of polymerization and T_g of the PIL is important to achieve the best combination of mechanical properties and ionic conductivity. Furthermore, optimizing the resin formula will be beneficial in developing a more robust, mechanically stable and conductive PIL based resin wafer.

4.3.3 Effect on Current Efficiency of the system

Figure 4-7 shows a comparison of average current efficiencies for PE-EDI and PIL-EDI runs. In all cases, current efficiencies were generally high with the exception of PE-EDI run at 8V and all PIL-EDI runs. The unusual increase in current efficiency above 100% can be attributed to potential fouling in the system caused by salt precipitating on the membrane or resin surface. Another reason for the higher than normal current efficiencies was ion leakage within

compartments (especially from concentrate compartments to the diluate compartments). A detailed analysis of current efficiency against final diluate feed volume is provided in the Appendix.

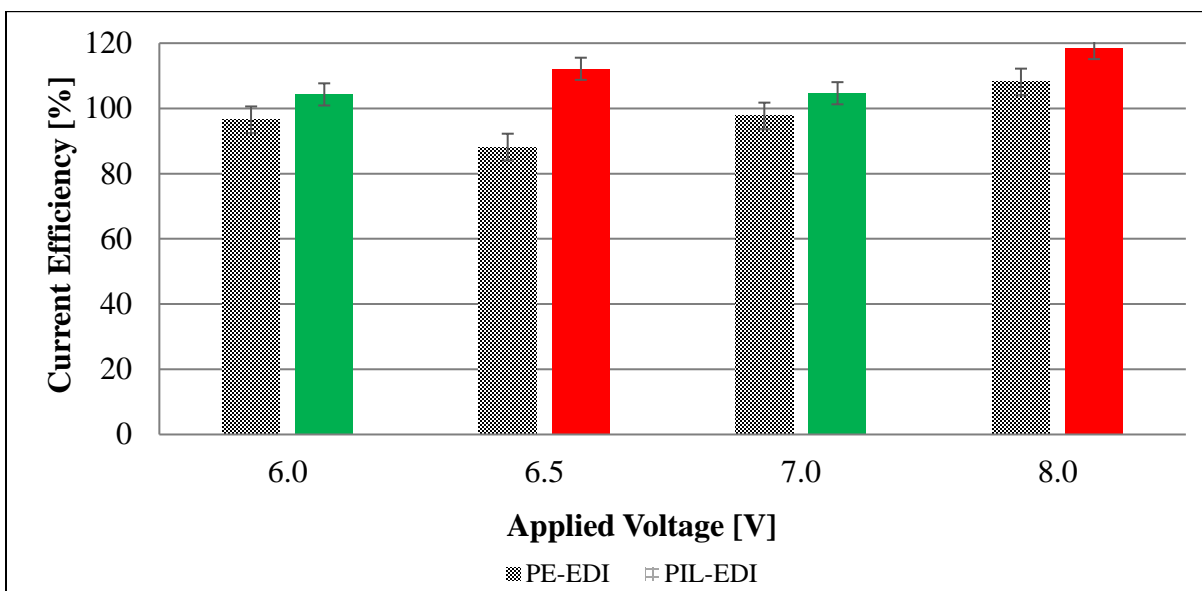


Figure 4-11: A comparison of average current efficiencies for PE-EDI and PIL-EDI runs. PIL-EDI (comprising 3.0 g PIL) is shown as red bars while PIL-EDI (comprising 2.5 g PIL) is shown as green bars.

CHAPTER 5

5. SUMMARY AND CONCLUSION

In this study, polyionic liquids were investigated for use in Resin Wafer Electrodeionization (RW-EDI). Phosphonium-based IL [P888VB][TF2N] was synthesized, polymerized and combined with dry resin mixture to form two variants of PIL-based resin wafer (PIL-RW), each with different PIL amounts. The mechanical properties, electrochemical properties, morphological characteristics and influence in EDI applications of the PIL-RW were examined and analyzed against conventional polyethylene-based resin wafers (PE-RW). The electrochemical impedance spectroscopy results showed that PIL-RW had a higher conductivity than PE-RW. The morphological characteristics revealed that PIL tended to coat the resin beads and reduce the active sites for ion transport. Coating of beads was more pronounced when a higher amount of PIL was used. The performances of PE-EDI, PIL-EDI (comprising 3.0 g PIL) and PIL-EDI (comprising 2.5 g PIL) were investigated for removal efficiency, current responses, and specific energy consumption (SEC). Generally, the differences in PE-EDI and PIL-EDI performance were more prominent when 2.5g PIL was used. The results showed that PIL-EDI (comprising 2.5 g IL) conducted more ions than PE-RW even at lower ionic concentrations. Another observation was that PIL-RW (comprising 2.5 g IL) displayed a higher removal rate than PE-RW. Furthermore, a lower SEC was achieved with PIL-EDI (comprising 2.5 g IL) than PE-EDI at relatively similar removal efficiencies. However, PIL conductivity and PIL-RW

formulation limited the extent of the improvement. It was concluded that balancing the degree of cure and glass transition of PIL was necessary to boost the electrochemical and mechanical properties in resin wafers. Finally, current efficiencies of both conventional and modified RW-EDI were generally high, except for some unusually high current efficiencies above 100% which were related to ion leakage and fouling in the system.

CHAPTER 6

6. FUTURE WORK

Although PIL proved to induce ion conductivity in resin wafer and improve SEC of the RW-EDI system, more experiments are required to further establish the hypothesis. Research into PIL properties, resin wafer formulation and EDI operating conditions would help achieve this and advance this study. The development of a PIL-based resin wafer that provides adequate mechanical support and prevents coating of resin beads would result in enhanced ion transport within the bed. Further investigations into phosphonium based or other different PIL materials may also provide insights into the the best combination of physical and conductive properties that will be suitable for resin wafer applications. Different resin wafer formulations will also need to be developed and evaluated to determine an optimal formula. This research could be conducted as a detailed design of experiments that considers both the material properties and system conditions.

LIST OF REFERENCE

- [1] TheWorldCounts, Water, water everywhere... but not a drop to drink, (2014).
<http://www.theworldcounts.com/stories/average-daily-water-usage>.
- [2] FAO, Water withdrawal and pressure on water resources, (2014).
<http://www.fao.org/nr/water/aquastat/didyouknow/index2.stm>.
- [3] A.M. Wachinski, Membrane Processes For Water Resuse, McGraw-Hill, 2013.
- [4] Global Water Intelligence, Global Water Report 2011, Oxford, UK, 2010.
- [5] Committee on Sustainable Water Supplies for the Middle East, WATER FOR THE FUTURE, NATIONAL ACADEMY PRESS, Washington, D.C, 1999. doi:10.17226/6031.
- [6] T. Track, G. Tel, Materials, Process & technology challenges for the vision 2050, (2011) 1–34.
- [7] R. Goldstein, W. Smith, Water & Sustainability: U.S. Electricity Consumption for Water Supply & Treatment - The Next Half Century, Water Supply. 4 (2002) 93. doi:10.1017/CBO9781107415324.004.
- [8] B. Dziegielewski, Strategies for Managing Water Demand, (2003) 29–39.
- [9] A. Gonzalez-Perez, K.M. Persson, Bioinspired materials for water purification, Materials (Basel). 9 (2016). doi:10.3390/ma9060447.
- [10] A. Richardson, US Wastewater Market To Total \$11B Through 2025, 2015.
<https://www.flowcontrolnetwork.com/us-wastewater-market-total-11b-2025/>.

- [11] R.W. Baker, Ion Exchange Membrane Processes – Electrodialysis, 2012. doi:10.1002/0470020393.ch10.
- [12] Li, Norman N. Fane, A.G. Ho, T. W.S. Winston Matsuura, Advanced Membrane Technology and Applications, John Wiley & Sons., 2008. <https://app.knovel.com/hotlink/toc/id:kpAMTA000A/advanced-membrane-technology/advanced-membrane-technology>.
- [13] J. Kucera, Desalination: Water from Water, 2014. doi:10.1002/9781118904855.
- [14] K. Mabry, City Seeks Public Input on New Recycled Water Program, (2011). <http://www.encino.patch.com/articles/city-seeks-public-input-on-new-recycled-water-program>.
- [15] T. and T.J. Pankratz, Deslination.com: An Environmental Primer, 2nd ed., Lone Oak Publishing, Houston, Texas, 2004.
- [16] R. Zhao, S. Porada, P.M. Biesheuvel, A. Van der Wal, Energy consumption in membrane capacitive deionization for different water recoveries and flow rates, and comparison with reverse osmosis, *Desalination*. 330 (2013) 35–41. doi:10.1016/j.desal.2013.08.017.
- [17] S.Y. Pan, S.W. Snyder, H.W. Ma, Y.J. Lin, P.C. Chiang, Energy-efficient resin wafer electrodeionization for impaired water reclamation, *J. Clean. Prod.* 174 (2018) 1464–1474. doi:10.1016/j.jclepro.2017.11.068.
- [18] S.S. Pan, L. Berkeley, S. Snyder, P. Chiang, Electrokinetic Desalination of Brackish Water and Associated Challenges in the Water and Energy Nexus, (2018). doi:10.1039/C7EW00550D.

- [19] J. Du, N. Lorenz, R.R. Beitle, J.A. Hestekin, Application of Wafer-Enhanced Electrodeionization in a Continuous Fermentation Process to Produce Butyric Acid with *Clostridium tyrobutyricum*, *Sep. Sci. Technol.* 47 (2012) 43–51. doi:10.1080/01496395.2011.618170.
- [20] S. Datta, Y.J. Lin, D.J. Schell, C.S. Millard, S.F. Ahmad, M.P. Henry, P. Gillenwater, A.T. Fracaro, A. Moradia, Z.P. Gwarnicki, S.W. Snyder, Removal of acidic impurities from corn stover hydrolysate liquor by resin wafer based electrodeionization, *Ind. Eng. Chem. Res.* 52 (2013) 13777–13784. doi:10.1021/ie4017754.
- [21] L. Xu, F. Dong, H. Zhuang, W. He, M. Ni, S.P. Feng, P.H. Lee, Energy upcycle in anaerobic treatment: Ammonium, methane, and carbon dioxide reformation through a hybrid electrodeionization–solid oxide fuel cell system, *Energy Convers. Manag.* 140 (2017) 157–166. doi:10.1016/j.enconman.2017.02.072.
- [22] S. Datta, M.P. Henry, Y.J. Lin, A.T. Fracaro, C.S. Millard, S.W. Snyder, R.L. Stiles, J. Shah, J. Yuan, L. Wesoloski, R.W. Dorner, W.M. Carlson, Electrochemical CO₂ Capture Using Resin-Wafer Electrodeionization, *Ind. Eng. Chem. Res.* 52 (2013) 15177–15186. doi:10.1021/ie402538d.
- [23] J.A. Hestekin, C.N. Hestekin, G.A. Morrison, S.A. Paracha, US20180093030A1, 2018.
- [24] J. Song, M. Song, K. Yeon, J. Kim, K. Lee, S. Moon, Purification of a primary coolant in a nuclear power plant using a magnetic filter – electrodeionization hybrid separation system, *262* (2004) 725–732.
- [25] L. Alvarado, A. Chen, Electrodeionization: Principles, strategies and applications, *Electrochim. Acta.* 132 (2014) 583–597. doi:10.1016/j.electacta.2014.03.165.

- [26] J.M. Bernatowicz, M.J. Snow, R.J. O'Hare, Methods and Apparatus for the Formation of Heterogeneous Ion Exchange Membranes, 6,503,957B1, 2003.
- [27] W. Su, R. Pan, Y. Xiao, X. Chen, Membrane-free electrodeionization for high purity water production, DES. 329 (2013) 86–92. doi:10.1016/j.desal.2013.09.013.
- [28] W. Su, T. Li, X. Jiang, X. Chen, Membrane-free electrodeionization without electrode polarity reversal for high purity water production, Desalination. 345 (2014) 50–55. doi:10.1016/j.desal.2014.04.018.
- [29] N. Si, Room-temperature ionic liquids: a novel versatile lubricant, (2001) 2244–2245. doi:10.1039/b106935g.
- [30] R.D. Noble, D.L. Gin, Perspective on ionic liquids and ionic liquid membranes, J. Memb. Sci. 369 (2011) 1–4. doi:10.1016/j.memsci.2010.11.075.
- [31] A.M. Lopez, J.A. Hestekin, Improved organic acid purification through wafer enhanced electrodeionization utilizing ionic liquids, J. Memb. Sci. 493 (2015) 200–205. doi:10.1016/j.memsci.2015.06.008.
- [32] J. Yuan, M. Antonietti, Poly(ionic liquid) latexes prepared by dispersion polymerization of ionic liquid monomers, Macromolecules. 44 (2011) 744–750. doi:10.1021/ma102858b.
- [33] X. Han, D.W. Armstrong, Ionic liquids in separations, accounts of chemical research, Acc. Chem. Res. 40 (2007) 1079–1086.
- [34] P. Chem, M. Antonietti, Polymer Chemistry Nitrogen-doped carbon fibers and membranes by carbonization of electrospun poly (ionic liquid) s †, (2011) 1654–1657. doi:10.1039/c1py00196e.

- [35] S. Zhang, K. Dokko, M. Watanabe, Porous ionic liquids: Synthesis and application, *Chem. Sci.* 6 (2015) 3684–3691. doi:10.1039/c5sc01374g.
- [36] D. Gromadzki, A. Jigounov, P. Št, Synthesis of thermally responsive cylindrical molecular brushes via a combination of nitroxide-mediated radical polymerization and “grafting onto” strategy, 46 (2010) 804–813. doi:10.1016/j.eurpolymj.2009.12.015.
- [37] L. Qin, B. Wang, Y. Zhang, L. Chen, G. Gao, hierarchical porous structure in poly (ionic liquid) s †, (2017) 3785–3788. doi:10.1039/c6cc10158e.
- [38] G.B. Appetecchi, G. Kim, M. Montanino, M. Carewska, R. Marcilla, D. Mecerreyes, I. De Meazza, Ternary polymer electrolytes containing pyrrolidinium-based polymeric ionic liquids for lithium batteries, *J. Power Sources.* 195 (2010) 3668–3675. doi:10.1016/j.jpowsour.2009.11.146.
- [39] B. Qiu, B. Lin, Z. Si, L. Qiu, F. Chu, J. Zhao, F. Yan, Bis-imidazolium-based anion-exchange membranes for alkaline fuel cells, *J. Power Sources.* 217 (2012) 329–335. doi:10.1016/j.jpowsour.2012.06.041.
- [40] J. Yuan, D. Mecerreyes, M. Antonietti, Poly(ionic liquid)s: An update, *Prog. Polym. Sci.* 38 (2013) 1009–1036. doi:10.1016/j.progpolymsci.2013.04.002.
- [41] O. Kuzmina, *Polymerized Ionic Liquids : Properties for Applications*, The Royal Society of Chemistry, 2018.

- [42] A.M. Lopez, M.G. Cowan, D.L. Gin, R.D. Noble, Phosphonium-Based Poly(ionic liquid)/Ionic Liquid Ion Gel Membranes: Influence of Structure and Ionic Liquid Loading on Ion Conductivity and Light Gas Separation Performance, *J. Chem. Eng. Data.* 63 (2018) 1154–1162. doi:10.1021/acs.jced.7b00541.
- [43] Segalman Group, POLYMERIC IONIC LIQUIDS, (n.d.).
<http://www.segalman.mrl.ucsb.edu/polymeric-ionic-liquids>.
- [44] K.-E. Bouhidel, A. Lakehal, Influence of voltage and flow rate on electrodeionization (EDI) process efficiency, *Desalin.* Bouhidel, A. Lakehal / *Desalin.* 193 (2005) 21–26. doi:10.1016/j.desal.2005.08.027.
- [45] Y. Ervan, I.G. Wenten, Study on the influence of applied voltage and feed concentration on the performance of electrodeionization, *Songklanakarin J. Sci. Technol.* 24 (2002) 955–963.
- [46] X.Y. Zheng, S.Y. Pan, P.C. Tseng, H.L. Zheng, P.C. Chiang, Optimization of resin wafer electrodeionization for brackish water desalination, *Sep. Purif. Technol.* 194 (2018) 346–354. doi:10.1016/j.seppur.2017.11.061.
- [47] S.-Y. Pan, S.W. Snyder, H.-W. Ma, Y.J. Lin, P.-C. Chiang, Development of a Resin Wafer Electrodeionization Process for Impaired Water Desalination with High Energy Efficiency and Productivity, *ACS Sustain. Chem. Eng.* 5 (2017) 2942–2948. doi:10.1021/acssuschemeng.6b02455.
- [48] P. Kollsman, *Electrodialytic Apparatus*, 2,689,826, 1954.
- [49] P. Kollsman, *Methods of and Apparatus for treating Ionic Fluids by Dialysis*, 2,815,320, 1957.

- [50] E. Glueckauf, Electrodeionization through a packed bed, *Br. Chem. Eng.* 4 (1959) 646–651.
- [51] Z. Matejka, No Title, *Appl. Chem. Biotechnol.* 21 (1971) 117.
- [52] S.S. Yoshida, Regeneration mechanism of ion exchange materials in electrodeionization, *Electrochemistry.* 70 (2002) 784–788.
- [53] H. MENG, C. PENG, S. SONG, D. DENG, Electro-Regeneration Mechanism of Ion-Exchange Resins in Electrodeionization, *Surf. Rev. Lett.* 11 (2005) 599–605. doi:10.1142/s0218625x04006542.
- [54] M.R.J. Wyllie, *Electrical potentials across porous plugs and membranes*, (1956).
- [55] M. Elimelech, W.A.W. Phillip, The future of seawater desalination: energy, technology, and the environment, *Science* (80-.). 333 (2011) 712–717. doi:10.1126/science.1200488.
- [56] D. Rathin, Lin YuPo, B. Dennis, Tsai Shih-Perng, Electrodeionization substrate, and device for electrodeionization treatment, 6495014, 2001.
- [57] Y.J. Lin, M.P. Henry, S.W. Snyder, E. St. Martin, M. Arora, L. de la Garza, (US), DEVICES USING RESIN WAFERS AND APPLICATIONS THEREOF, 7,507,318 B2, 2009.
- [58] K.H. Yeon, J.H. Song, S.H. Moon, Preparation and characterization of immobilized ion exchange polyurethanes (IEPU) and their applications for continuous electrodeionization (CEDI), *Korean J. Chem. Eng.* 21 (2004) 867–873. doi:10.1007/BF02705532.
- [59] J.W. Lee, K.H. Yeon, J.H. Song, S.H. Moon, Characterization of electroregeneration and determination of optimal current density in continuous electrodeionization, *Desalination.* 207 (2007) 276–285. doi:10.1016/j.desal.2006.04.070.

- [60] B. Lin, S. Cheng, L. Qiu, F. Yan, S. Shang, J. Lu, Protic Ionic Liquid-Based Hybrid Proton-Conducting Membranes for Anhydrous Proton Exchange Membrane Application, (2010) 1807–1813. doi:10.1021/cm9033758.
- [61] M. Ambrogi, G.A. Tiruye, D. Cordella, K. Grygiel, Innovative polyelectrolytes / poly (ionic liquid) s Fátima N Ajjan , a Martina Ambrogi , b Girum Ayalneh Tiruye , c, (2017). doi:10.1002/pi.5340.
- [62] M. Chen, B.T. White, C.R. Kasprzak, T.E. Long, Advances in phosphonium-based ionic liquids and poly(ionic liquid)s as conductive materials, *Eur. Polym. J.* 108 (2018) 28–37. doi:10.1016/j.eurpolymj.2018.08.015.
- [63] H.G.D.J.R.M.C.E.B.J.E. McGrath, Main-chain poly(arylene ether) phosphonium ionomers, *Appl. Organomet. Chem.* 12 (1988) 781–785.
- [64] B. Pospiech, Application of Phosphonium Ionic Liquids as Ion Carriers in Polymer Inclusion Membranes (PIMs) for Separation of Cadmium(II) and Copper(II) from Aqueous Solutions, *J. Solution Chem.* 44 (2015) 2431–2447. doi:10.1007/s10953-015-0413-2.
- [65] A.C. Barsanti, C. Chiappe, T. Ghilardi, C.S. Pomelli, RSC Advances Functionalized phosphonium based ionic liquids : properties and application in metal extraction, (2014) 38848–38854. doi:10.1039/c4ra04723k.
- [66] T. Ho, Ion selective removal using wafer-enhanced electrodeionization, University of Arkansas, 2007.

APPENDIX

Experiment Set 1

Vol 0.5 L

V 6.5 V

Q 150 mL/min 0.15 L/min

N 2 RW 2

PIL-EDI																	
PE-EDI						PIL-EDI											
1			2			3			1			2			3		
Current (A)	Dil (g/L)	CE (%)	Current (A)	Dil (g/L)	CE (%)	Current (A)	Dil (g/L)	CE (%)	Current (A)	Dil (g/L)	CE (%)	Current (A)	Dil (g/L)	CE (%)	Current (A)	Dil (g/L)	CE (%)
0.14	4.13	0.00	0.14	3.90	0.00	0.14	4.44	0.00	0.11	6.15	0.00	0.11	6.93	0.00	0.12	7.50	0.00
0.13	3.62	42.90	0.13	3.69	18.15	0.12	3.62	77.97	0.00	0.00	0.00	0.00	0.00	0.00	0.00	0.00	0.00
0.12	2.80	37.87	0.11	2.61	51.51	0.11	2.96	34.43	0.09	6.66	29.90	0.10	6.35	42.88	0.10	5.78	55.16
0.09	2.13	24.04	0.08	1.89	28.96	0.09	2.18	33.00	0.09	5.28	58.17	0.09	5.26	44.16	0.08	4.74	44.14
0.07	1.49	23.11	0.06	1.35	22.20	0.07	1.72	19.05	0.08	4.37	30.79	0.08	4.24	34.07	0.08	3.93	28.89
0.05	0.99	19.01	0.05	0.91	18.35	0.05	1.11	27.76	0.07	3.29	32.97	0.07	3.43	24.95	0.07	2.98	29.11
0.03	0.57	19.96	0.03	0.57	16.24	0.04	0.76	16.99	0.06	1.67	47.55	0.06	1.80	47.78	0.06	1.52	42.98
0.02	0.31	17.50	0.02	0.27	19.28	0.03	0.48	15.01	0.05	1.23	13.25	0.05	1.43	10.91	0.05	1.12	11.83
									0.04	0.92	9.75	0.04	1.03	12.84	0.04	0.89	7.39
									0.03	0.69	8.42	0.03	0.84	6.82	0.03	0.69	7.18
(%)		73.74	CE (%)		75.50	CE (%)		78.65	CE (%)		96.23	CE (%)		116.17	CE (%)		124.38
RE		92.60	RE (%)		93.03	RE (%)		89.18	RE (%)		88.79	RE (%)		87.83	RE (%)		90.81
R (Ω)		80.00	R (Ω)		83.87	R (Ω)		80.00	R (Ω)		80.00	R (Ω)		78.79	R (Ω)		77.61
SEC (kWh/kg)		2.02	SEC (kWh/kg)		1.97	SEC (kWh/kg)		1.89	SEC (kWh/kg)		1.55	SEC (kWh/kg)		1.28	SEC (kWh/kg)		1.20
SEC (kWh/m3)		0.46	SEC (kWh/m3)		0.43	SEC (kWh/m3)		0.45	SEC (kWh/m3)		0.51	SEC (kWh/m3)		0.47	SEC (kWh/m3)		0.49

Experiment Set 2

Vol 0.5 L

V **8 V**

Q 150 mL/min 0.15 L/min

N 2 RW 2

Time (h)	PE- EDI									PIL-EDI									
	1			2			3			1			2			3			
	Current (A)	Dil (g/L)	CE (%)	Current (A)	Dil (g/L)	CE (%)	Current (A)	Dil (g/L)	CE (%)	Current (A)	Dil (g/L)	CE (%)	Current (A)	Dil (g/L)	CE (%)	Current (A)	Dil (g/L)	CE (%)	
0	0.21	5.41	0.00	0.22	4.99	0.00	0.24	6.02	0.00	0.16	7.29	0.00	0.16	7.29	0.00	0.15	6.99	0.00	
1	0.18	4.35	62.26	0.19	3.60	77.69	0.21	4.29	88.11	0.15	6.41	64.67	0.15	6.14	87.62	0.14	5.77	96.02	
2	0.14	2.89	52.21	0.14	2.31	44.89	0.15	2.65	52.29	0.13	4.93	60.46	0.13	4.79	59.55	0.12	4.55	53.98	
3	0.09	1.81	36.09	0.09	1.46	28.28	0.09	1.42	39.26	0.11	3.73	38.36	0.11	3.65	37.77	0.10	3.42	39.15	
4	0.07	1.14	23.81	0.07	0.91	19.49	0.07	0.80	22.00	0.09	2.87	24.50	0.08	1.84	54.49	0.08	1.78	52.26	
5	0.05	0.76	14.70	0.05	0.64	10.58	0.05	0.51	10.95	0.07	1.35	43.66	0.07	1.51	10.13	0.07	1.49	8.82	
6	0.04	0.55	8.58	0.04	0.43	8.70	0.05	0.40	4.49	0.05	0.90	14.39	0.06	1.20	9.05	0.07	1.30	5.17	
7	0.03	0.44	5.46	0.04	0.36	2.82	0.04	0.35	1.59	0.05	0.87	0.86	0.05	0.93	8.13	0.06	1.15	3.79	
	CE (%)	85.89	CE (%)	82.94	CE (%)	85.47	CE (%)	120.95	CE (%)	121.19	CE (%)								
	RE (%)	91.93	RE (%)	92.76	RE (%)	94.14	RE (%)	88.06	RE (%)	87.23	RE (%)								
	R (Ω)	79.01	R (Ω)	76.19	R (Ω)	71.11	R (Ω)	79.01	R (Ω)										
	SEC (kWh/kg)	2.13	SEC (kWh/kg)	2.21	SEC (kWh/kg)	2.14	SEC (kWh/kg)	1.52	SEC (kWh/kg)	1.51	SEC (kWh/kg)								
	SEC (kWh/m ³)	0.64	SEC (kWh/m ³)	0.61	SEC (kWh/m ³)	0.73	SEC (kWh/m ³)	0.58	SEC (kWh/m ³)										

Experiment Set 4

Vol 0.5 L

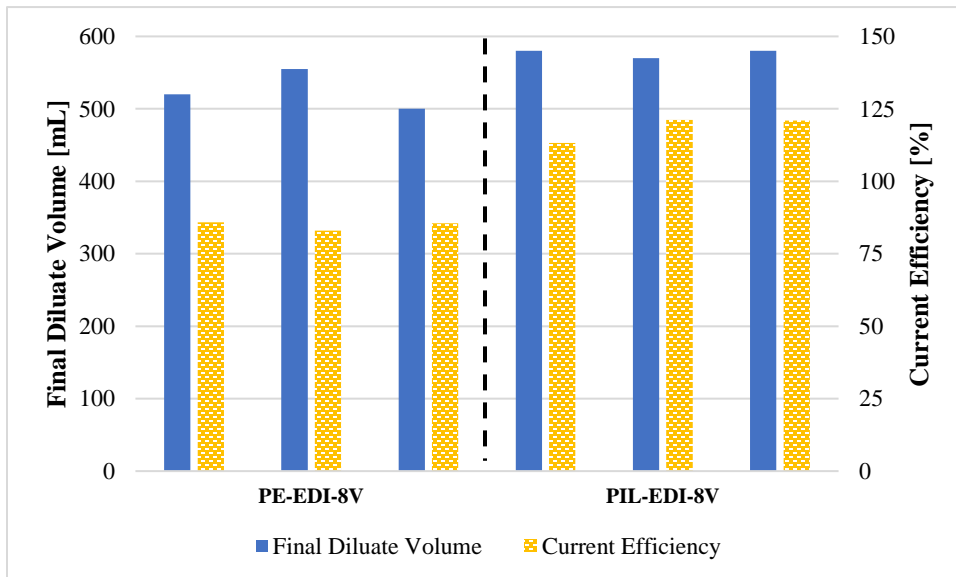
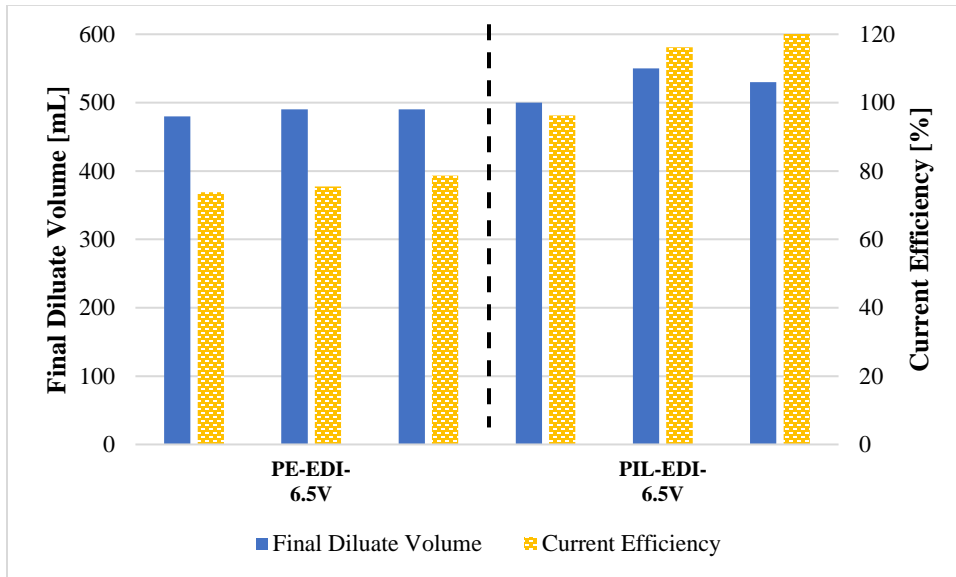
V **7 V**

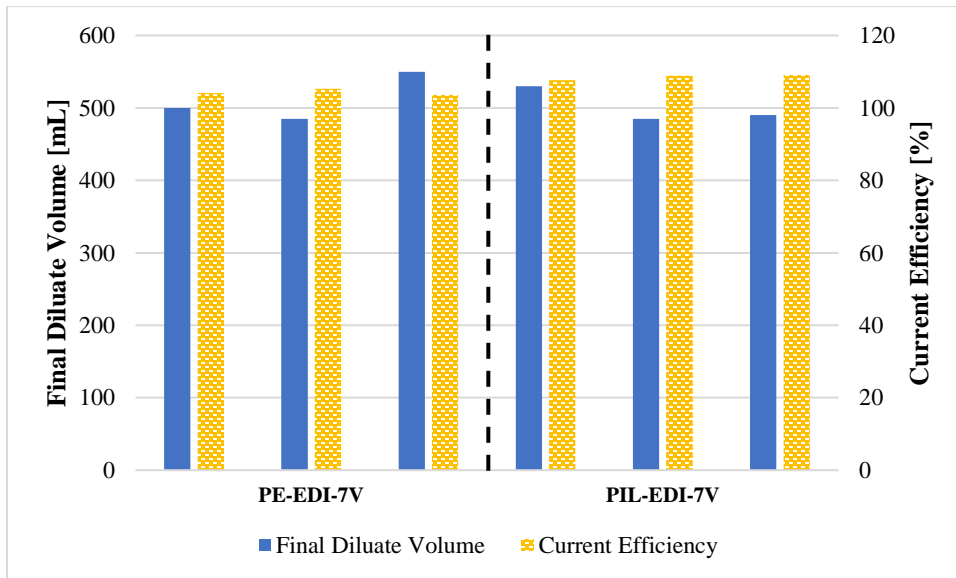
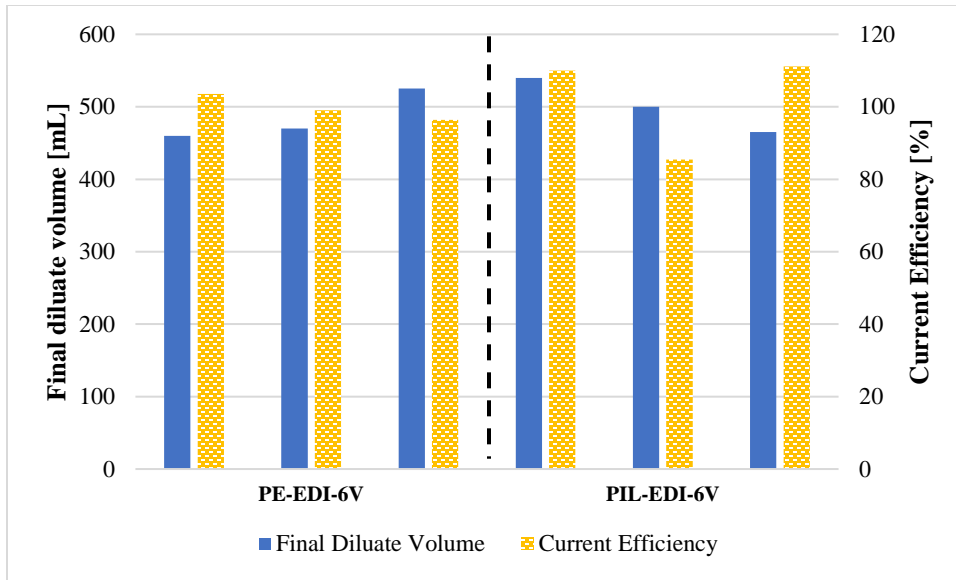
Q 150 mL/min 0.15 L/min

N 2 RW 2

Time (h)	PE-EDI									PIL-EDI								
	1			2			3			1			2			3		
	Current (A)	Dil (g/L)	CE (%)	Current (A)	Dil (g/L)	CE (%)	Current (A)	Dil (g/L)	CE (%)	Current (A)	Dil (g/L)	CE (%)	Current (A)	Dil (g/L)	CE (%)	Current (A)	Dil (g/L)	CE (%)
	1			2			3			1			2			3		
0	0.14	5.36	0.00	0.14	5.56	0.00	0.14	5.57	0.00	0.13	6.03	0.00	0.14	6.01	0.00	0.14	6.23	0.00
1	0	0.00	0.00	0.00	0.00	0.00	0.00	0.00	0.00	0.00	0.00	0.00	0.13	3.63	202.14	0.00	0.00	0.00
2	0	0.00	0.00	0.00	0.00	0.00	0.13	3.73	77.97	0.00	0.00	0.00	0.12	1.56	94.94	0.00	0.00	0.00
3	0	0.00	0.00	0.00	0.00	0.00	0.00	0.00	0.00	0.00	0.00	0.00	0.00	0.00	0.00	0.00	0.00	0.00
4	0	0.00	0.00	0.00	0.00	0.00	0.00	0.00	0.00	0.09	1.35	121.96	0.00	0.00	0.00	0.09	1.23	124.33
5	0.06	0.66	107.66	0.06	0.61	113.32	0.00	0.00	0.00	0.07	0.80	15.59	0.06	0.47	27.80	0.00	0.00	0.00
6	0.04	0.38	10.92	0.03	0.29	13.65	0.04	0.38	75.26	0.00	0.00	0.00	0.00	0.00	0.00	0.00	0.00	0.00
7	0.03	0.13	-6.19	0.02	0.08	13.72	0.00	0.00	0.00	0.04	0.24	16.81	0.02	0.04	17.67	0.02	0.11	33.39
8	0.02	0.04	5.13	0.01	0.01	6.36	0.02	0.06	15.35	0.03	0.14	4.14	0.00	0.00	0.00	0.01	0.01	9.68
CE (%)	104.16			105.31			103.62			107.64			108.89			109.04		
RE (%)	99.20			99.77			98.98			97.71			99.41			99.82		
R (Ω)	120.69			134.62			84.85			97.22			74.47			107.69		
SEC (kWh/kg)	1.54			1.52			1.55			1.49			1.47			1.47		
SEC (kWh/m ³)	0.49			0.51			0.51			0.53			0.53			0.55		

Appendix B





VITAE

Angela Fasuyi

Oxford MS | **Email:** ajibolafasuyi@gmail.com

Education

- 2017- 2019 M.S. Chemical Engineering | University of Mississippi, Oxford MS
- 2012- 2015 B.Eng. Chemical Engineering (Hons) | University of Manchester, United Kingdom

Academic Appointments

Jan 2017- May 2019 **Graduate Research and Teaching Assistant** | Department of Chemical Engineering, University of Mississippi, Oxford MS

- Research Project: Investigations into Ionic Liquid Functionalized Ion Exchange Resin Wafer for low energy Electrodeionization.
- Teaching Assistant for ‘Fluid Dynamics’ and ‘Heat Transfer-Plant Design’ courses.

Professional Experience

Oct 2018 – June 2019 **Project Engineer** | Saratoga Energy Resources, Houston, TX

- Professionally interfaced with OEM, subcontractors, technical team and client to deliver turnkey project successfully.
- Assisted team lead with the development of the project scope, cost and schedule.
- Collaborated with cross functional leadership team to drive productivity.
- Managed Engineering, Procurement, Installation for the repair of ExxonMobil QIT Mobiltherm Fired Heater.

Jun-Aug 2018

Chemical Engineering Intern (Downstream Chemicals) | Baker

Hughes, a GE Company, Sugarland TX

- Improved efficiency of Petroleum and Fuel Additives (PFA) Group's digital workspace and supported knowledge management initiatives.
- Assisted PFA Technology Support team with product application survey on the field.
- Utilized Hansen Solubility Program to resolve Contaminant Extraction Service (CES) challenges.
- Conducted key 'No-Harms' tests on emerging sulfur reduction products.
- Developed PFA Quality Documents and SOPs for key product testing methods as part of the company's quality assurance efforts.

Dec 2015- Nov 2016 **Project Engineer** | Harrowgate Energy Services

- Worked and liaised with OEMs, vendors, internal leadership and key stakeholders to ensure successful delivery of projects and manage the expectations of the stakeholders.
- Managed Engineering, Procurement, and Installation of \$200,000 Shell Bonga Floating Production Storage and Offloading (FPSO) Fire & Gas System Upgrade and executed cost analysis to reduce procurement costs by \$12,000.
- Worked with a team of 5 to produce proposals/bids for contracts.
- Responsible for implementation of Quality Management System of the company and its services.
- Managed the establishment and implementation of the Harrowgate Training Centre Project.
- Directly supervised Health Safety & Environment programs in the office by conducting safety inspections, induction and training of staff that led to a low injury frequency rate of less than 5% every quarter.

Skills

- **General/Soft Skills:** Problem Solving, Quality Management System, Data Analysis, Database Management, Time Management, Verbal/Written Communication, Team Collaboration, Attention to detail.
- **Software:** Proficient in the use of Microsoft Office Suite, HYSYS, MATLAB, PYTHON. Ability to quickly learn new software systems and deliver quality output with acquired skill.

Recent Certification/Training

- Mar 2016 **PECB** ISO 9001 Quality Management System Lead Auditor Course
- May 2016 **IFP School** MOOC Oil & Gas (Exploration to Distribution)
- June 2016 **NEBOSH** International General Certificate in Occupational Health & Safety
- July 2018 **Houston Area Safety Council** (Basic Plus)

Professional Affiliation(s)

Member - American Institute of Chemical Engineers (AIChE)

Member - National Society of Black Engineers

Conference Presentations

Fasuyi, A., Lopez, A. “Design of Ionic Liquid Epoxy Functionalized Ion Exchange Resin Wafers for Low-energy Electrodeionization”. The 8th Annual Research Symposium, University of Mississippi, Oxford, MS, U.S.A. March 21- (2018).

Fasuyi, A., Lopez, A. “Design of Ionic Liquid Epoxy Functionalized Ion Exchange Resin Wafers for Low-energy Electrodeionization”. Annual Meeting of the American Institute of Chemical Engineers (AIChE), Minneapolis, MN, U.S.A. October 29 - November 3 (2017).

Fasuyi, A., Lopez, A. “Design of Ionic Liquid Epoxy Functionalized Ion Exchange Resin Wafers for Low-energy Electrodeionization”. The 3rd Annual UM/UMMC Research Day, University of Mississippi, Oxford MS, USA. April 13th- (2017).

Honors and Activities

- Won the Second Prize in the STEM poster session at the 8th Annual Research Symposium organized by the UM Graduate Student Council, University of Mississippi, Oxford, MS, USA. March 21-(2018).
- Scholarship for graduate studies, University of Mississippi, Oxford, Mississippi, USA (Jan 2017-Aug 2019).
- Treasurer of the African Caribbean Student Association (ACSA) of the University of Mississippi (Aug 2017-Dec 2017).
- Academic (Merit-Based) Scholarship of £4000 from Liverpool John Moores University (2011)

Interest / Extracurricular Activities

Emerging Technology, Current Global Affairs, Watching Documentaries and Fact videos,

Personal Fitness & Group sports, Volunteering at a local Hospice center, Travelling, Adventures.